A Study of the Globular Cluster NGC 7089 Using RR Lyrae Distance Measurements

By:

Russell Zimmerman

An honors thesis submitted in partial fulfillment of the requirements for the bachelor of science degree in physics.

Advisor: Dr. David Sukow

Dept Head: Dr. Irina Mazilu

Collaborator: Michael Fitzgerald OSS

Submitted April 2022

Washington and Lee University
Russell Zimmerman class of 2022

Abstract

Globular clusters are gravitationally bound groups of stars averaging about 13 billion years old. Since the universe itself is around 14 billion years old, globular clusters can give valuable insight into the formation history of galaxies. A significant percentage of the stars making up globular clusters are RR Lyrae variable stars. These stars' pulsation periods are measured in order to determine the star's distance to Earth. In this study 14 RR Lyrae variable stars from globular cluster NGC 7089 (M2) are measured using 1 meter Sinistro telescopes accessed through Las Cumbres Observatory's network of robotic telescopes. From these measurements a distance estimate of NGC 7089 to earth is found to be 11.48kpc. I also provide evidence that NGC 7089 is an Oosterhoff II cluster through examination of average RRab pulsation period, r value, metallicity, and age of the cluster.

Introduction to RR Lyrae Stars

Distance in the universe is measured by astronomers using a type of cosmological ladder. This ladder has various "rungs" where each rung is a range of distance away. Each rung has certain types of measurements necessary to obtain accurate distance measurements depending on how far away the celestial objects are in each rung. The first few rungs are mainly determined using parallax, proper motion of stars, and main sequence fitting, all of which are beyond the scope of this paper. The next rung of the ladder, which measures stars between about 100 to 10^7 parsecs away, is made using variable star measurements[1]. These stars are referred to as standard candles. Standard candles are objects with a known absolute magnitude. Equation 1 is used to calculate distance from apparent and absolute magnitudes[2].

$$d = 10^{\frac{m-M-A+5}{5}} pc \quad (1)$$

The known absolute magnitude, M, is related to the observed magnitude, m, and the extinction factor, A, to get a calculated distance between the observer and the celestial object[3]

There are two main types of stars with a determinable absolute magnitude, RR Lyrae and Cepheid. These are variable star types which have the critical relationship between their pulsation period and their absolute magnitude. Cepheid stars usually have a pulsation period between 1 to 70 days. Because of this, acquiring enough telescope time to track their entire pulsation periods is unfeasible within the duration of my particular study. RR Lyrae, on the other hand, have pulsation periods ranging from about .2 to 1 day. Pulsation within the RR Lyrae stars is caused by their nuclear chemistry. Pulsation is caused by a mechanical motion of matter within the star. The basics of the cause behind this are that as the star compresses, photons increase the pressure within the star due to being trapped. This causes a volume expansion of the star, which in turn releases energy in the way of photons. This decreases the pressure and the star is then compressed by gravity, restarting the pulsation. This is referred to as the Kappa Mechanism[4]. There is much more to discuss about why variable stars pulsate, however, this is not within the realm of this paper.

What is important is the relationship between an RR Lyrae star's pulsation period, and its absolute magnitude. For certain filters used to view the RR Lyrae star, there is a direct relationship between pulsation period and absolute magnitude. The absolute magnitude of the entire spectrum of the star, called the absolute bolometric magnitude, is the ideal quantity to determine. This value is calculated theoretically by the equation below[5].

$$m_{bol} = -2.5 log_{10}\left(\int_0^\infty F_\lambda d\lambda\right) + C_{bol} \quad (2)$$

[1] "Modern Cosmological Observations and Problems - G. Bothun."
[2] Carroll and Ostlie, *An Introduction to Modern Astrophysics*.
[3] Cardelli, Clayton, and Mathis, "The Relationship between Infrared, Optical, and Ultraviolet Extinction."
[4] Fitzgerald, "Course."
[5] Carroll and Ostlie, *An Introduction to Modern Astrophysics*.

Where $F_\lambda d\lambda$ is the monochromatic flux, and C_{bol} is a bolometric constant at a given filter. The monochromatic flux is governed by the equation below[6].

$$F_\lambda d\lambda = \frac{L_\lambda}{4\pi r^2} d\lambda \qquad (3)$$

The bolometric constant, C_{bol}, will vary depending on the filter used. Though the absolute bolometric magnitude is ideal, it is not easy to calculate using current telescopes. Instead, the absolute magnitude of the star is found between specific wavelength bandwidths. The filters I used to determine absolute magnitude were visible (V), infrared (i), and zed (z). The midpoint wavelength of V is 544.8nm with a bandwidth of 84nm. The midpoint wavelength of infrared is 798nm with a bandwidth of 154nm. The midpoint wavelength of zed is 870nm with a bandwidth of 104nm[7]. The luminosity magnitudes at each wavelength are also dependent on a sensitivity function, $S(\lambda)$. The sensitivity function is dependent on the telescope, and is modeled as a near step function. Figure 1 displays an example of the sensitivity function of the Sloan telescope[8].

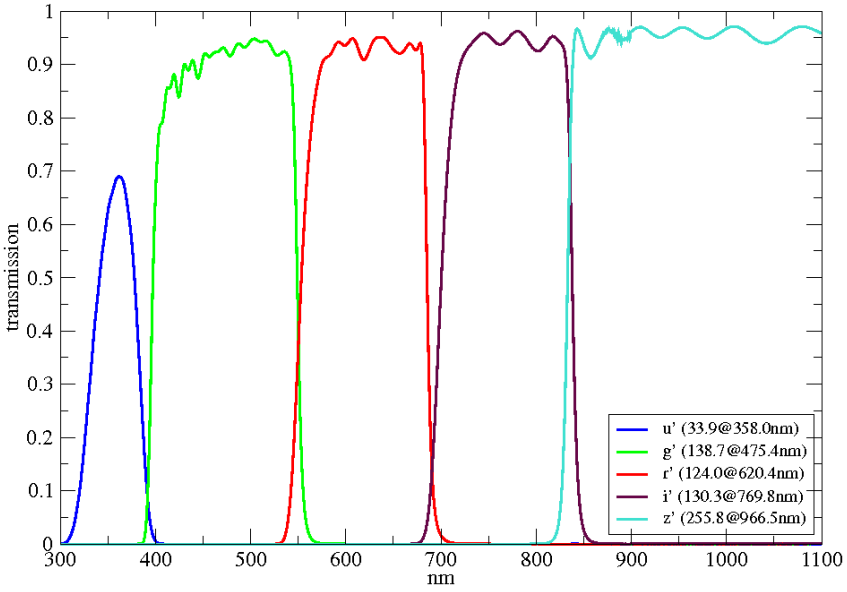

Figure 1: Graph of sensitivity function of the Sloan telescope.

Using this, a theoretical model is used to calculate the expected absolute magnitude at each wavelength[9].

$$U = -2.5log_{10}\left(\int_0^\infty F_\lambda S(\lambda)\right) + C_U \qquad (4)$$

[6] Carroll and Ostlie.
[7] "LCO Filters Documentation."
[8] Granzer, "Sloan u'g'r'i'z' Filter Curves — English."
[9] Carroll and Ostlie, *An Introduction to Modern Astrophysics*.

This is the approach to determine the absolute magnitude of ANY star. RR Lyrae stars, however, have a periodicity to absolute magnitude dependency, factoring in metallicity. The dependency of the three filters I used can be seen below in equations 5[10], 6 and 7[11].

$$M_V = 2.288 + 0.882\, log_{10}(Z) + 0.108(log_{10}(Z))^2 \quad (5)$$

$$M_i = 0.908 - 1.035\, log_{10}(P) + 0.220 log_{10}(Z) \quad (6)$$

$$M_z = 0.839 - 1.295\, log_{10}(P) + 0.211 log_{10}(Z) \quad (7)$$

From these, Z is a relationship dependent on the metallicity of the star, and P is the measured pulsation period. Note that the visible spectrum relies only on metallicity, while the i and z spectra rely on both metallicity and periodicity. Metallicity is the measurement of elements composing a star that are heavier than hydrogen and helium, and is obtained from the spectra of the star[12]. For my purpose I used the metallicity value determined by [Fe/H]. For [Fe/H], the ratio of atoms of iron to atoms of hydrogen is compared to the base ratio of iron to hydrogen which is set to be the sun's. Using these ratios, a value for [Fe/H] is calculated[13].

$$[Fe/H] = log_{10}\left[\frac{(N_{Fe}/N_H)_{star}}{(N_{Fe}/N_H)_{\odot}}\right] \quad (8)$$

N represents the number of atoms per unit mass. Using [Fe/H] the Z value is calculated[14].

$$log(Z) = 0.977[Fe/H] - 1.699 \quad (9)$$

The pulsation period for an RR Lyrae star is calculated using a plot of its apparent brightness vs phase. Since the periods of RR Lyraes are on the order of hours, enough data points cannot be collected during a single pulsation to create an accurate brightness vs phase diagram. Instead a collection of points are used from a collection of different pulsations of the same star. Software is then used to "fold" these points all onto the same pulsation period axis. This is done in order to create an accurate model of a single pulsation. There are a variety of techniques to measure the actual period of a star based off of this plot. A relatively simple, yet effective, method is the string-length method. The idea behind this method is to ask the question "how much string does it take to connect all the points on the plot using the least amount of string?". This question is answered computationally by "guessing" a string length, and then seeing if that string length is a reasonable minimization. A reasonable string length is between 1.0 to 2.0 normalized units, based on a knowledge of a star's range of possible periods. The most accurate string length is determined by other factors depending on the computational software used[15]. This string length is

---

[10] Catelan, Pritzl, and Smith, "The RR Lyrae Period-Luminosity Relation. I. Theoretical Calibration."
[11] Cáceres and Catelan, "The Period-Luminosity Relation of RR Lyrae Stars in the SDSS Photometric System."
[12] Fitzgerald, "Course."
[13] "FeHcalculator.Pdf."
[14] Cáceres and Catelan, "The Period-Luminosity Relation of RR Lyrae Stars in the SDSS Photometric System."
[15] Dworetsky, "A Period-Finding Method for Sparse Randomly Spaced Observations or "How Long Is a Piece of String?"

then used to calculate the period of pulsation. In Fig 2 we can see an example of an apparent brightness vs phase plot of an RR Lyrae star[16].

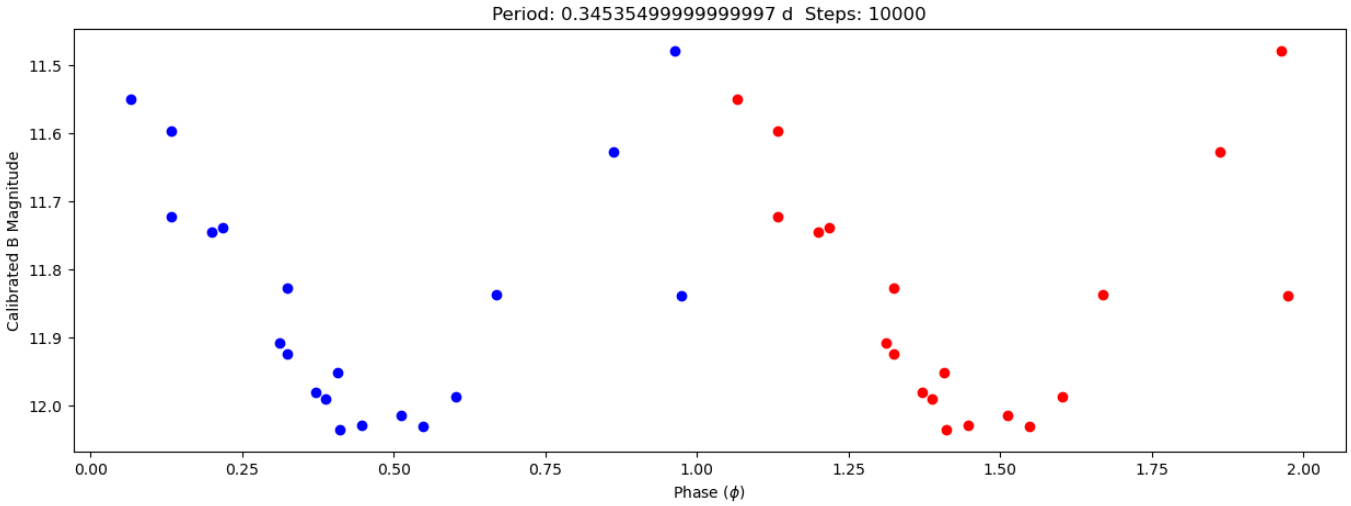

Figure 2: Calibrated apparent magnitude vs phase plot of RR Lyrae star OZ UMa. Period is calculated to be about .345 days using the string length method.

The vertical axis shown in fig 2 is the apparent magnitude of the star. For my study, these values are determined computationally by comparing the amount of light received from the target star and the amount of light received by other non-variable comparison stars of known magnitudes within the image. Finally the extinction factor, A, must be determined. There is a certain amount of astronomical dust between the star and the observer. This dust causes extinction in the form of reddening. Redding is caused by scattering of photons upon hitting the dust. Since redder wavelengths have an easier time passing through without being scattered, their intensity is diminished less than the bluer wavelengths. This means that bluer light will be viewed as dimmer than redder light. This must be accounted for in order to determine equal distances to the same star for any filter. To do this a color excess, defined as $E(B-V)$ must be used to appropriately scale the apparent magnitudes for each filter. The extinction factor and the color excess are related below[17].

$$A_{\lambda} = R * E(B-V) \qquad (10)$$

The R value is different based on different forms of absorption and scattering. Within the Milky Way the R value is 3.1 for the visible spectra. However, this R value will vary slightly with varying filters to account for reddening. We now have everything required to determine a distance calculation.

[16] Zimmerman, Bakhtadze, and Dorogy, "New Distance and Period Estimates to OZ UMa, an RR Lyrae Star."
[17] Carroll and Ostlie, *An Introduction to Modern Astrophysics*.

Categorization of RR Lyrae Stars

RR Lyrae stars are designated into three groups: types ab, c, and d. These classifications are defined by the stars' mode of pulsation. Type RRab stars are defined as pulsating in the fundamental mode[18]. RRab stars are observed to be more red, have steeper magnitude vs phase curves, and longer periods (>.5 days)[19]. RRab Lyrae stars have also been empirically measured to have a Blazhko occurrence rate of about 47%[20]. The Blazhko effect is the observed phenomena of amplitude and period variation of an RR Lyrae star. Modulation periods, how long it takes for the period itself to complete an entire cycle due to the Blazhko effect, have been measured to range from 2 days to 2000 days[21]. Although there are a few hypotheses as to the cause of this phenomena, there is no definitive agreed upon cause. A plot of an RRab curve can be seen in Fig 3[22].

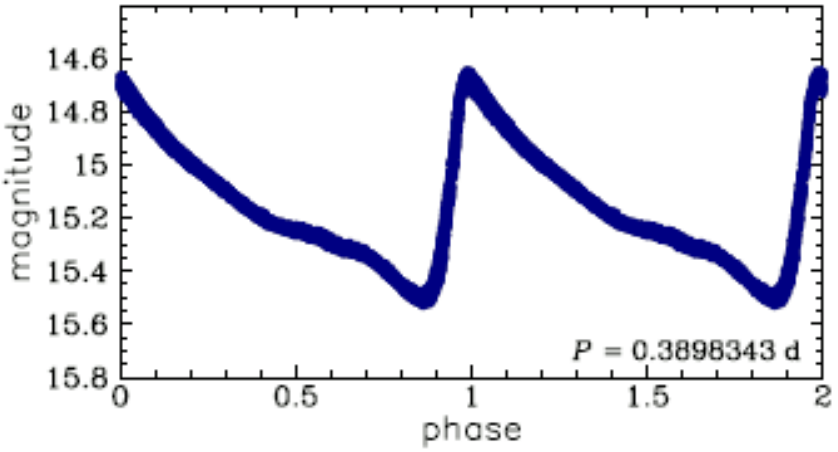

Figure 3: Magnitude vs phase plot of an unknown RRab type Lyrae star. This is an exception where the period is less than .5 days.

Type RRc Lyrae stars pulsate in the first-overtone mode. RRc Lyrae stars are observed to be bluer, have sinusoidal shaped magnitude vs phase curves, and have shorter periods (0.2 to 0.5 days)[23]. The Blazhko effect is also found to occur in RRc Lyrae stars with a much lower occurrence rate. As of 2018 the largest portion of RRc stars found to be Blazhko stars was 5.6% (607 out of 10826)[24]. See Fig 2 for an example of an RRc Lyrae type star curve.

---

[18] "OGLE Atlas of Variable Star Light Curves - RR Lyrae Stars."
[19] Fitzgerald, "Course."
[20] Jurcsik et al., "The Konkoly Blazhko Survey."
[21] Netzel et al., "Blazhko Effect in the First Overtone RR Lyrae Stars of the OGLE Galactic Bulge Collection."
[22] "OGLE Atlas of Variable Star Light Curves - RR Lyrae Stars."
[23] Fitzgerald, "Course."
[24] Netzel et al., "Blazhko Effect in the First Overtone RR Lyrae Stars of the OGLE Galactic Bulge Collection."

Type RRd Lyrae stars pulsate in the fundamental and the first-overtone mode. These are the rarest types of RR Lyrae stars and make up only about 0.5% of the RR Lyrae stars in metal-rich areas and about 10% in metal-poor areas. The periods of RRd stars do not vary widely, ranging between .74days to .75days. RRd Blazhko stars have been recorded, but are very difficult to find given the rarity of RRd Lyrae stars themselves. RRd Lyrae magnitude vs phase plots are broadened due to the interference between the fundamental and first-overtone modes. An example of this is seen in Fig. 4[25].

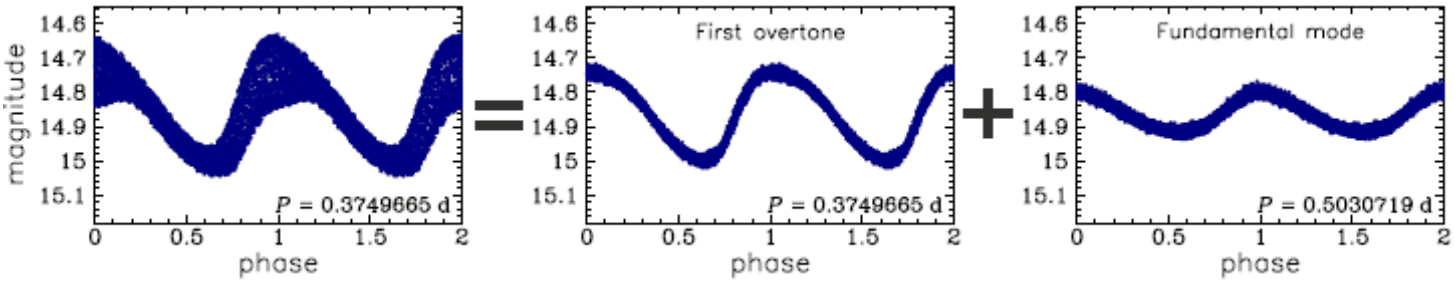

Figure 4: First-overtone portion of magnitude vs phase plot for unknown RRd Lyrae type star (middle). Fundamental mode portion of magnitude vs phase plot for unknown RRd Lyrae type star (right). Combined magnitude vs phase plot for unknown RRd Lyrae star (left).

RR Lyrae Evolution

RR Lyrae stars begin their lives as slightly smaller than the sun, roughly between .65$M_{\odot}$ and 1$M_{\odot}$. At the beginning of their evolution RR Lyrae stars lie on the main sequence of the Hertzsprung-Russell diagram at around 6000K and 1$L_{\odot}$. At this stage, along with all other main sequence stars, a future RR Lyrae star is undergoing nuclear fusion of hydrogen atoms to produce helium. The next stage of an RR Lyrae's evolution is moving onto the red giant branch of the HR diagram. The star is fusing hydrogen in a shell around a helium center. As more and more helium is produced and pushed into the core of the star, the RR Lyrae star grows. This growth increases the star's luminosity while maintaining a relatively constant temperature. While the star is growing to a larger and larger red giant it will eventually reach a point where the pressure in the core is so high that the helium will fuse together. This fusion results in the production of carbon, nitrogen, and oxygen. This is called the "Helium Flash". This will push the RR Lyrae star down and to the left of the HR diagram onto the horizontal branch (Fitzgerald). The first stages of an RR Lyrae evolution can be seen in Fig 5[26]. Along the horizontal branch all stars have relatively the same initial mass and a flat trend when temperature vs absolute magnitude is plotted, such as in Fig 6[27]. At this evolutionary point in a star's life, about 11-13 billion years old, is when we define it to be an RR Lyrae type star[28]. At this point the RR Lyraes have temperatures between 6000K and 7260K, with an absolute visual magnitude of around +0.6[29]. Along the horizontal branch of the HR diagram is an area called the instability strip.

---

[25] "OGLE Atlas of Variable Star Light Curves - RR Lyrae Stars."
[26] "Astronomy 1101."
[27] "Horizontal Branch - Wikipedia."
[28] Fitzgerald, "Course."
[29] Catelan, Pritzl, and Smith, "The RR Lyrae Period-Luminosity Relation. I. Theoretical Calibration."

Along this strip is where all pulsating stars, such as RR Lyrae and Cepheids, dwell. RR Lyrae are among the cooler and less bright of these stars, which can be seen in Fig 7[30].

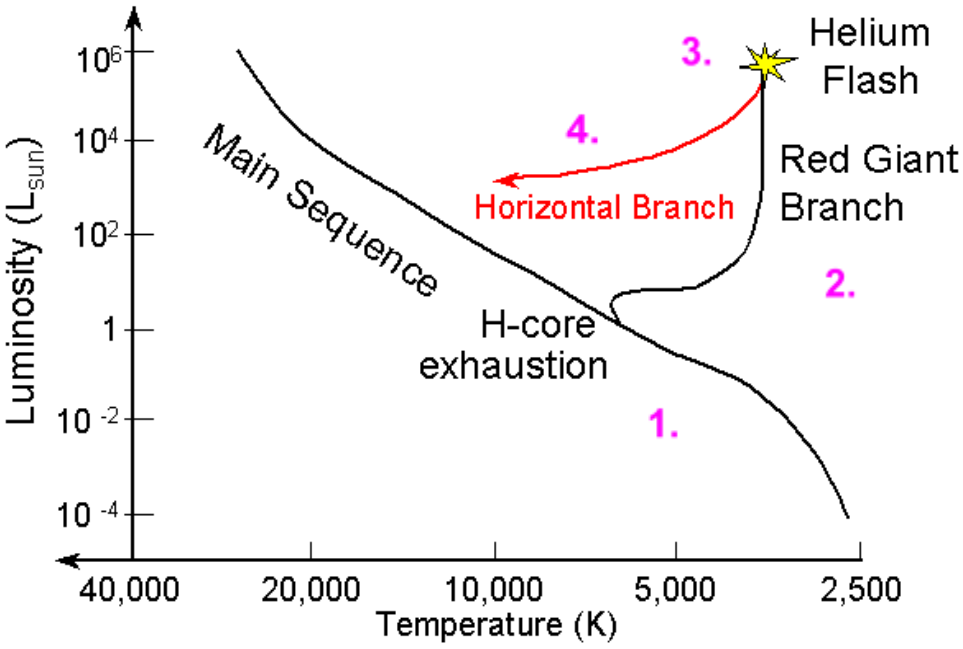

Figure 5: Hertzsprung-Russell diagram labeling the first four stages of an RR Lyrae star's life cycle. Stage 1 labeling the main sequence. Stage 2 labeling hydrogen shell fusion along red giant branch. Stage 3 labeling the helium flash. Stage 4 labeling placement along horizontal branch.

[30] "Instability Strip."

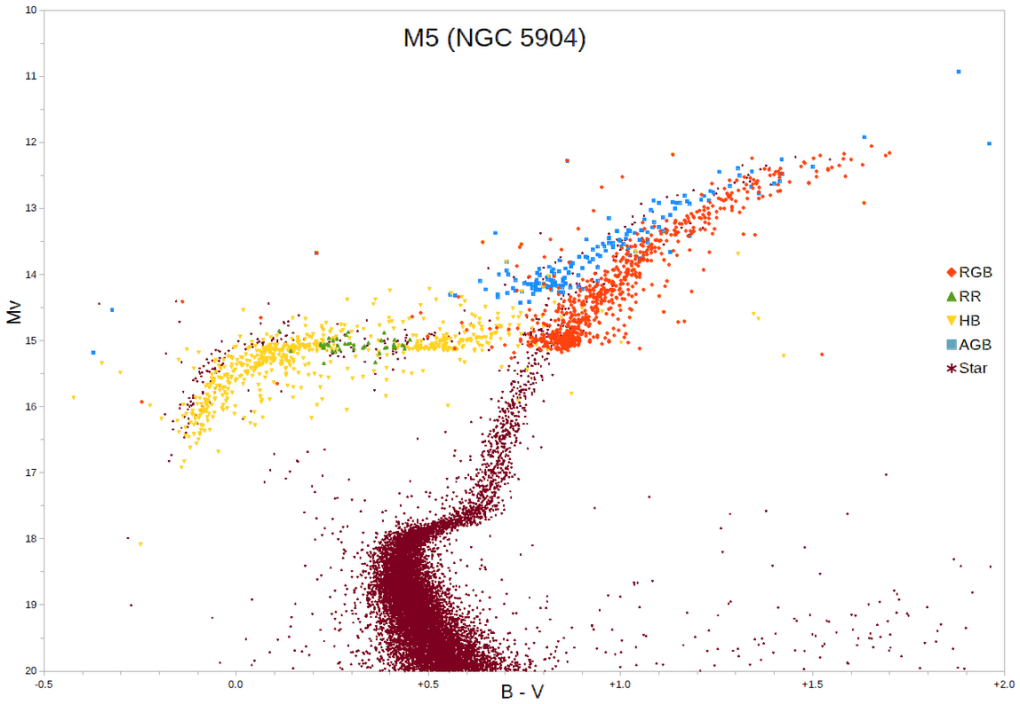

Figure 6: B-V vs absolute magnitude in V filter of a collection of stars within globular cluster NGC 5904. The horizontal branch can be seen as the yellow and green colored points. B-V is a way to express the temperature of a star.

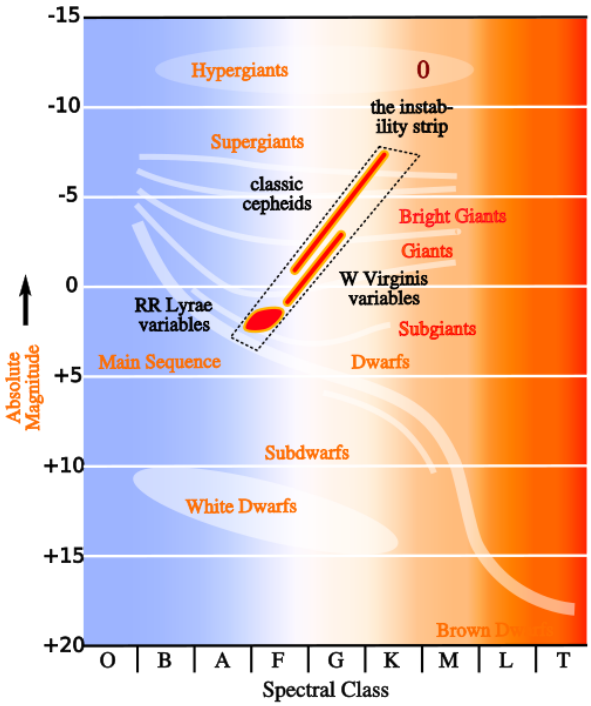

Figure 7: HR diagram including the location of the instability strip. RR Lyrae stars are labeled in the lower left of the instability strip.

RR Lyrae Relation to Globular Clusters

The close relationship between RR Lyrae stars and globular clusters is the reason for discussing the former within this paper. A globular cluster is defined as a relatively spherically symmetric group of older stars located in the halo of galaxies. The age of globular clusters are generally around 13 billion years old. Since the age of the universe is estimated to be about 14 billion years old, globular clusters' relative closeness in age to the universe itself makes them especially important within the sub-field of cosmology[31]. Distance measurements for Milky Way globular clusters can range between from about 4 to 123 kiloparsecs, with the mode being in the range of 6-12 kiloparsecs[32]. This makes distance measurements using parallax, proper motion, and main sequence fitting impossible with humanity's current telescope capabilities. Instead, astronomers can use variable stars, such as RR Lyraes, to determine distance measurements. This is an ideal measurement technique as RR Lyrae stars are abundant within globular clusters. Distance measurements for a collection of RR Lyrae stars are averaged and used to determine the distance of the globular cluster itself.

Globular Cluster General Properties

There are over 150 known galactic and extragalactic globular clusters. The galactic clusters create a halo around the Milky Way Galaxy. Globular clusters have relatively low metallicities. Globular cluster [Fe/H] metallicities range from about -0.23 to about -2.3[33]. Globular clusters contain between 100,000 and 1 million stars. Masses of globular clusters range from about $5M_{\odot}$ to over $1{,}000{,}000M_{\odot}$. Their diameters range from between 10 to 300 light years across. Although not commonly visible to the human eye, evident from their low apparent luminosity magnitudes due to their high distances, the absolute magnitudes of globular clusters are very high[34]. Absolute magnitudes of globular clusters range from about -1.0 to as high as -10, with a mode ranging from -6.5 to -8.5[35]. An average solar density of 2 stars per cubic light year, coupled with the existence of very bright stars making up a significant portion of globular clusters, are the causes of such high absolute magnitudes. Radial velocities of globular clusters have been determined using doppler shift analysis to range from NGC 6934's -411 kilometers per second to NGC 3201's +494 kilometers per second. These high velocities indicate that globular clusters have highly elliptical orbits around the galactic center[36].

Designation of types of globular clusters is dominated by the Oosterhoff classification system. There are three types of globular clusters under this classification system: Oosterhoff I, Oosterhoff II, and Oosterhoff III. As Oosterhoff III type globular clusters are extremely rare, understudied, and highly debated, I will be omitting a section regarding them[37]. The three main qualities that distinguish Oosterhoff types are the age of the cluster, the metallicity of the cluster, and the periodicity of the RRab Lyrae stars within the cluster. This paper will later focus heavily on how RR Lyrae stars factor into Oosterhoff type categorization.

---

[31] Fitzgerald, "Course."
[32] Harris, "A Catalog of Parameters for Globular Clusters in the Milky Way."
[33] Harris.
[34] "Globular Cluster | Astronomy | Britannica."
[35] Harris, "A Catalog of Parameters for Globular Clusters in the Milky Way."
[36] "Globular Cluster | Astronomy | Britannica."
[37] Fitzgerald, "Course."

Oosterhoff type I globular clusters are referred to as the "young halo"[38]. Globular clusters of this type are found to be mostly younger than 13 billion years old. [Fe/H] metallicities of type I clusters are seen to be greater than -1.6 labeled as "metal-rich"[39]. Average periodicities of RRab Lyrae stars of type I clusters are observed to be .54 days[40].

Oosterhoff type II globular clusters are referred to as the "old halo"[41]. Globular clusters of this type are found to be mostly older than 13 billion years old. Interestingly, NGC 7089 is an Oosterhoff II that actually disobeys this rule, which I will discuss later. [Fe/H] metallicities of type II clusters are seen to be less than -1.6, labeled as "metal-poor"[42]. Average periodicities of RRab Lyrae stars of type II clusters are observed to be .64 days.

An empirical relationship of the average log of each type's RRab periodicities can be seen in the equations below[43].

$$< log_{10}\left(P_I\right) > \; = \; -0.285 \pm 0.016 \quad (11)$$

$$< log_{10}\left(P_{II}\right) > \; = \; -0.250 \pm 0.012 \quad (12)$$

A correlation exists between the pulsation period of RRab Lyrae stars and the average fraction of RRc Lyrae stars within a cluster, denoted as "r". The r value is modeled empirically by equations below[44].

$$< r_I > \; = \frac{N_c}{N_{ab}+N_c} \; = 0.18 \pm 0.09 \quad (13)$$

$$< r_{II} > \; = \frac{N_c}{N_{ab}+N_c} = \; 0.49 \; \pm \; 0.09 \quad (14)$$

Using these relationships, coupled with data showing periodicities of RRab Lyrae stars within globular clusters, it is determined that RRab stars within Oosterhoff type II clusters are either more massive or more helium rich than type I RRab stars[45]. An empirical graph of the number of RRab Lyrae stars with various periodicities in type I and II clusters can be seen in Fig 8[46].

[38] Kuehn et al., "RR Lyrae in the LMC."
[39] van den Bergh, "Some Systematics of Galactic Globular Clusters."
[40] Stobie, "On the Difference Between the Oosterhoff Types i and II Globular Clusters."
[41] Kuehn et al., "RR Lyrae in the LMC."
[42] van den Bergh, "Some Systematics of Galactic Globular Clusters."
[43] Stobie, "On the Difference Between the Oosterhoff Types i and II Globular Clusters."
[44] Stobie.
[45] Stobie.
[46] Clement et al., "Variable Stars in Galactic Globular Clusters."

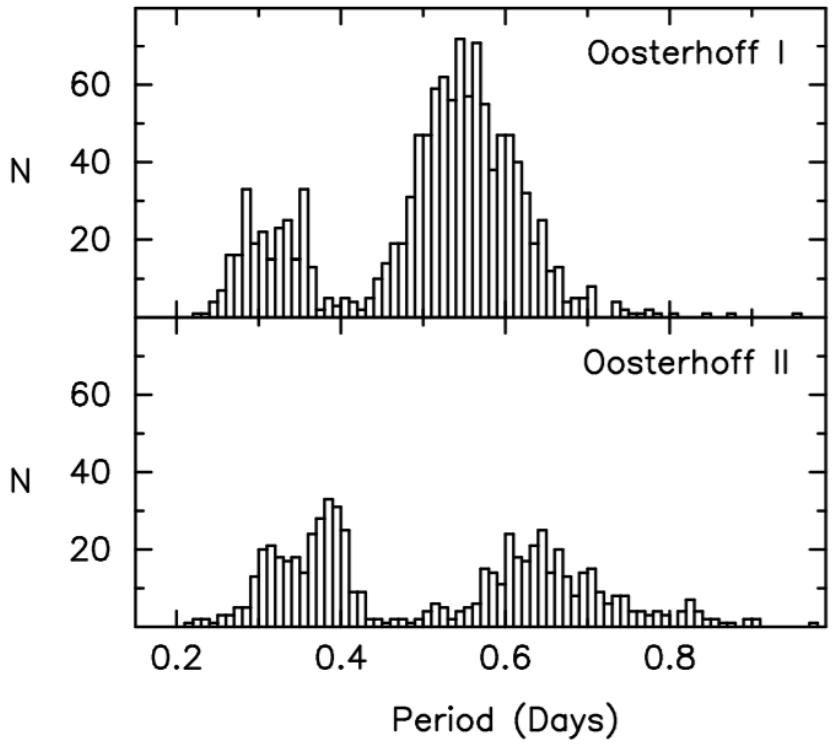

Figure 8: Bar graph relating number of RRab stars (N) to their periods in Oosterhoff I vs Oosterhoff II globular clusters.

A phenomenon observed between Oosterhoff I and Oosterhoff II globular clusters is the Oosterhoff gap. The Oosterhoff gap is the observed vacant area in the average RRab pulsation periods vs metallicities of globular clusters. The stark vacancy is interesting itself, however, what is more interesting is that this observed Oosterhoff gap is only present within Milky Way globular clusters. Discovering more about the Oosterhoff gap can glean insight into the creation of our galaxy. Fig 9 shows the side by side comparison of the existence of the Oosterhoff gap within Milky Way clusters compared to extragalactic clusters[47].

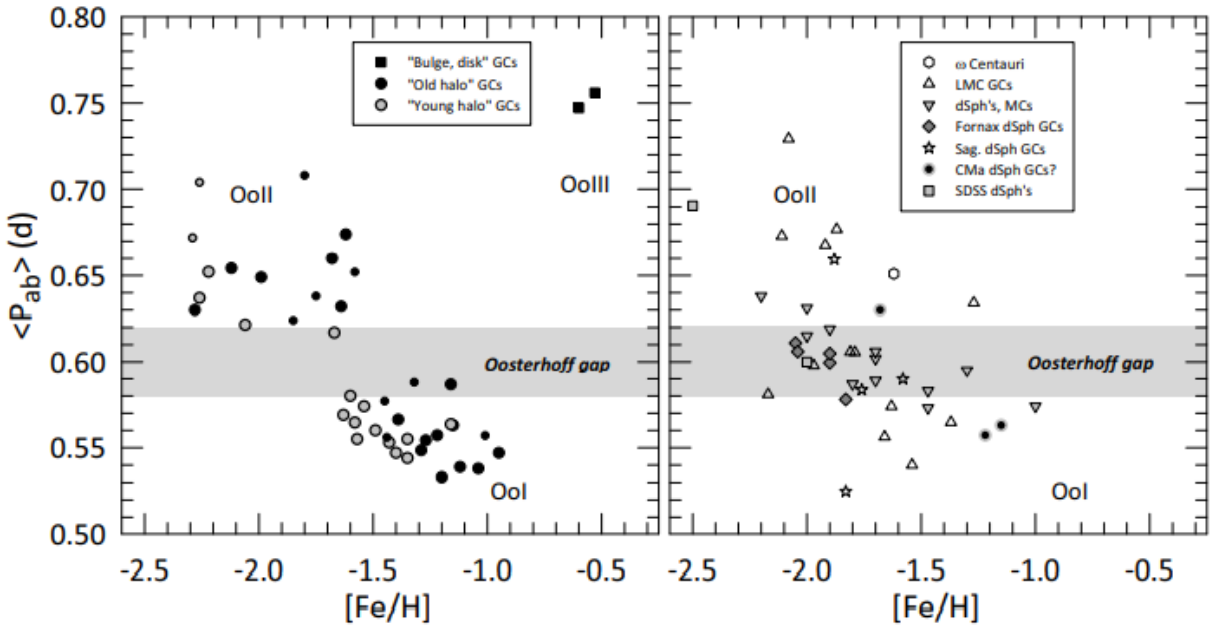

Figure 9: Plot of metallicity vs average pulsation period of RRab Lyrae stars for globular clusters within the Milky Way (left), and extragalactic globular clusters (right).

Methods

To choose an optimal globular cluster for this study, I looked at a few key qualities. Obviously, I needed the cluster to be visible within the timeframe of the data collection portion of this thesis project. I also required that the cluster have a previously published record of a collection of RR Lyrae stars to compare my data against. Lastly, it was essential that the cluster had a published metallicity, and preferably a published color excess value as well. Using the Las Cumbres Observatory visibility calculator, the catalog summaries of the Clement[48] and Harris[49] globular cluster data papers, I was able to select NGC 7089 (Messier 2) as an ideal candidate. Next, exposure times (time that the telescope spends collecting light from source) had to be calculated for each filter. Using Las Cumbres Observatory I ordered a 25 second Bessell-V filter

[47] Kuehn et al., "RR Lyrae in the LMC."
[48] Clement et al., "Variable Stars in Galactic Globular Clusters."
[49] Harris, "A Catalog of Parameters for Globular Clusters in the Milky Way."

test image of NGC 7089 using a 0.4 meter SBIG telescope. Using Aladin Sky Atlas I calculated exposure times of 30 seconds, 30 seconds, and 90 seconds for filters V, i, and z, respectively. These were calculated on the basis of ensuring a source-sky luminosity ratio between 10,000 and 50,000. On November 3rd, a two week long simple period cadence was ordered using LCO's 1.0 meter Sinistro telescope.

I reviewed the images to ensure they would provide accurate results when used as input for the data reduction. Images are unusable if they are out of focus to the point where the individual stars appear to have a hollow center, if the individual stars are oblong due to wind blowing on the telescope, or if the image is too blurry or blocked due to overcast. After tossing out about 10 images in each filter, a total of about 65 images were used for period calculation. A total of 57 RR Lyrae stars gathered from the SIMBAD database were chosen to be analyzed. To obtain light curves from the RR Lyrae stars the program "Astrosource" was used. Astrosource is an Astropy (astronomy python) based system designed by Our Solar Siblings[50]. Of the 57 stars analyzed by Astrosource, 14 had enough viable images sufficient for calculation. I will make a note here for anyone wishing to replicate the process I performed for a globular cluster that is more than 10kpc away using a 1m telescope or smaller. Due to the high density of stars, and the distance away, individual stars are difficult to discern by Astropy based code. For reference an example image from my data set can be seen in Fig 10.

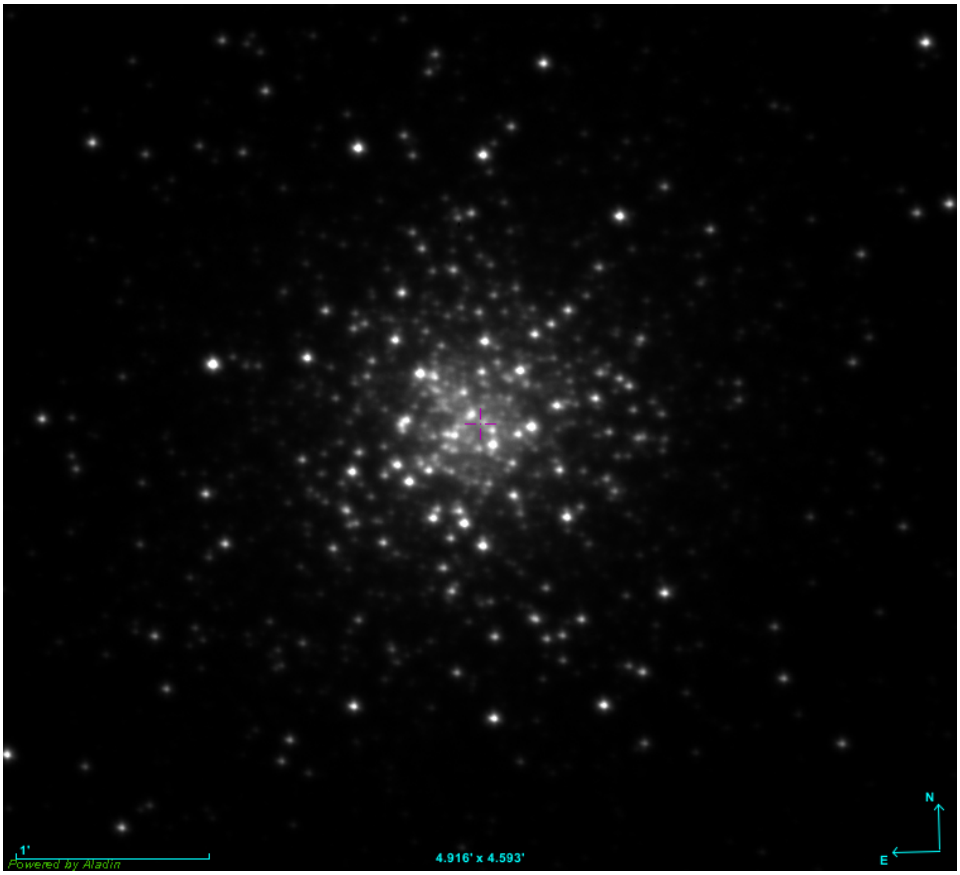

Figure 10: Image of NGC 7089 shot from LCO telescope and extracted via Aladin Sky Atlas.

[50] Fitzgerald, "Course."

To account for this, it is necessary to find the exact RA and Dec from the image for each RR Lyrae star down to about 8 decimal places in order to keep the center of the star within the scope of what the code is analyzing. A system to reject images that are not within a given apparent brightness is beneficial. Also a system where the scope of the code has a small radius of a few decimal points of RA and Dec is beneficial to make sure the star you want is always in frame (sometimes the star can be out of frame very slightly due to wind).

Data

Astrosource produces apparent luminosity vs phase diagrams derived from using both phase dispersion minimization as well as the string length method described earlier. For my data the string length method derived graphs are less noisy, so I have chosen to use them to calculate distance. Figures 11 through 13 show the V, i, and z apparent luminosity vs phase diagrams for star 1 (S1). Due to steep curves and a period above .5 days, I determine S1 to be RRab. Figure 13 displays an irregular double period due to an outlier image that the algorithm did not reject. This is a product of the computational software and not a reflection of the star's behavior.

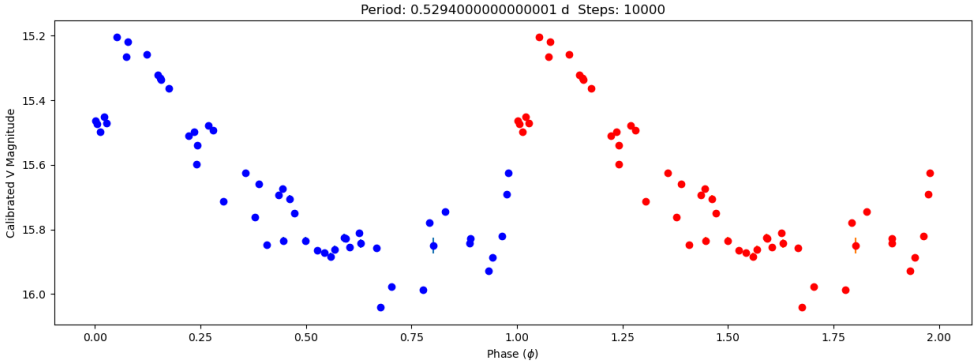

Figure 11: Apparent magnitude vs phase of V filter of S1.

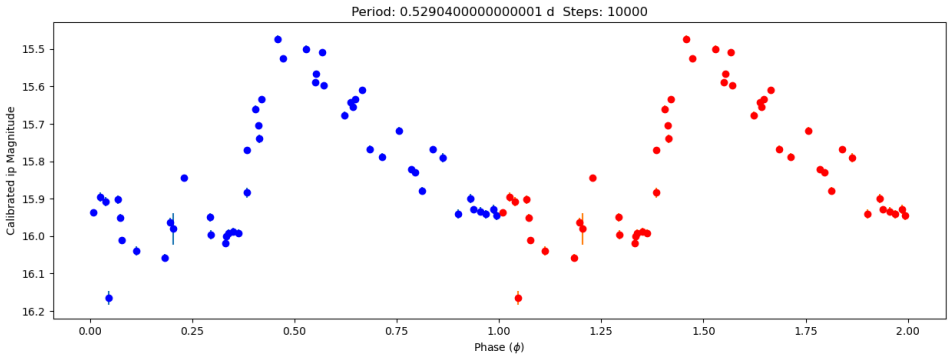

Figure 12: Apparent magnitude vs phase of i filter of S1.

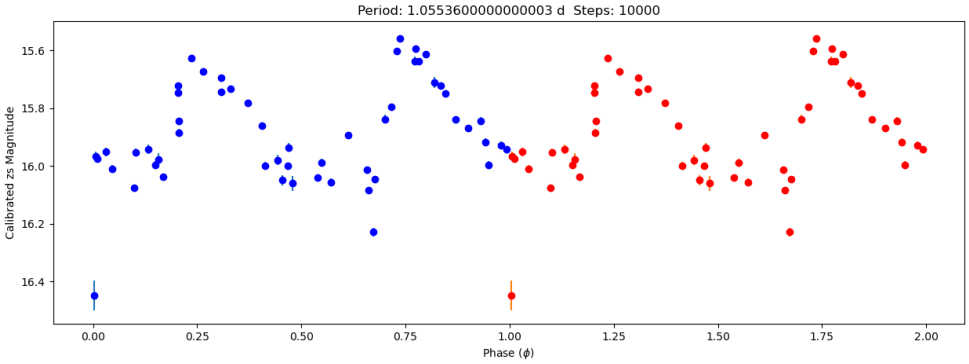

Figure 13: Apparent magnitude vs phase of z filter of S1.

Figures 14 through 16 show the V, i, and z apparent luminosity vs phase diagrams for S2. Due to steep curves and a period above .5 days, I determine S2 to be RRab.

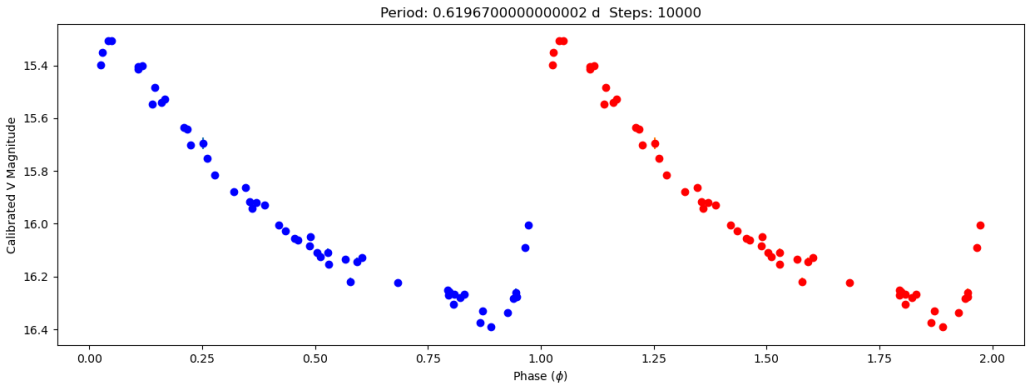

Figure 14: Apparent magnitude vs phase of V filter of S2.

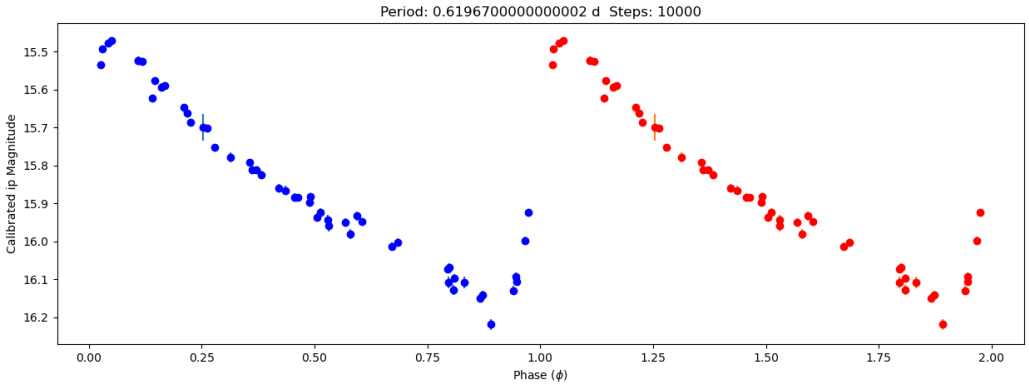

Figure 15: Apparent magnitude vs phase of i filter of S2.

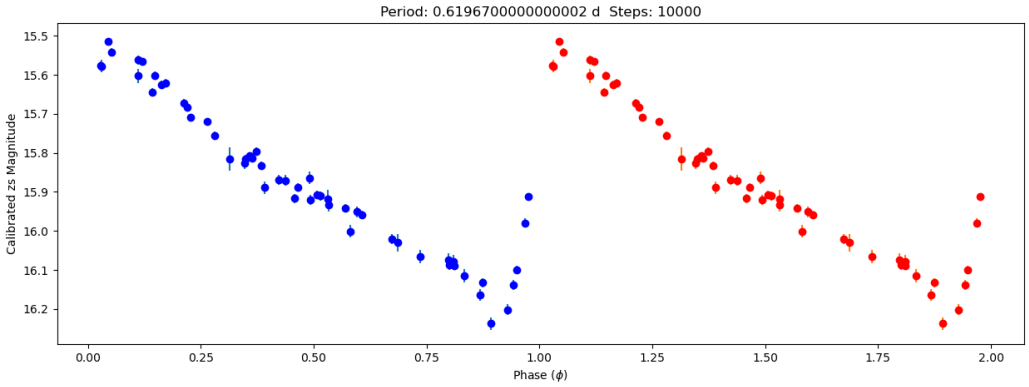

Figure 16: Apparent magnitude vs phase of z filter of S2.

Figures 17 through 19 show the V, i, and z apparent luminosity vs phase diagrams for S3. Due to steep curves and a period above .5 days, I determine S3 to be RRab.

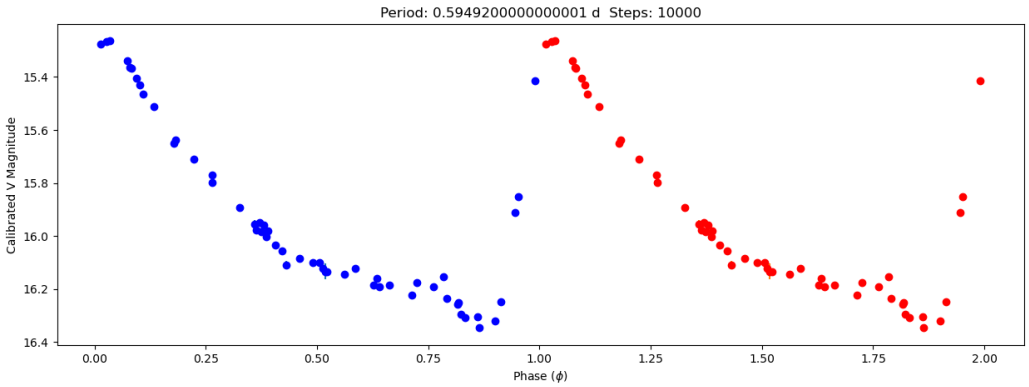

Figure 17: Apparent magnitude vs phase of V filter of S3.

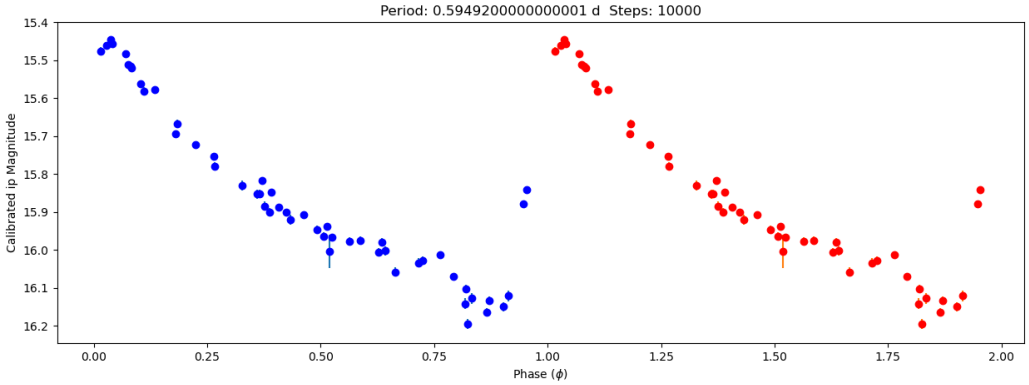

Figure 18: Apparent magnitude vs phase of i filter of S3.

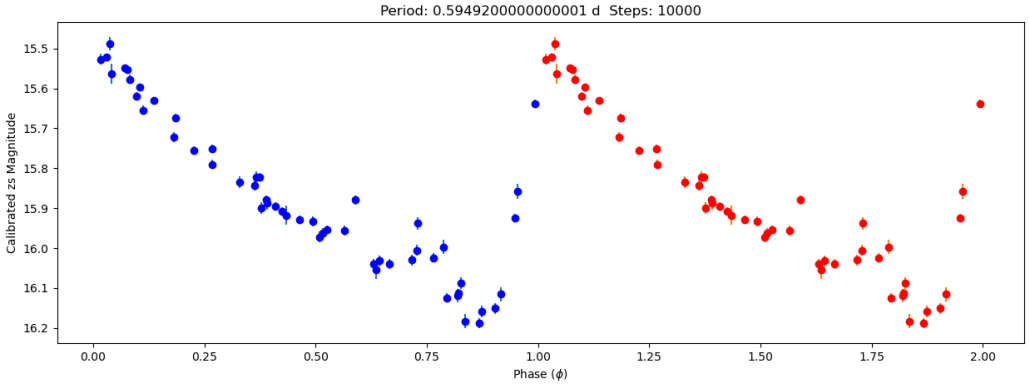

Figure 19: Apparent magnitude vs phase of z filter of S3.

Figures 20 through 22 show the V, i, and z apparent luminosity vs phase diagrams for S4. Due to steep curves and a period above .5 days, I determine S4 to be RRab.

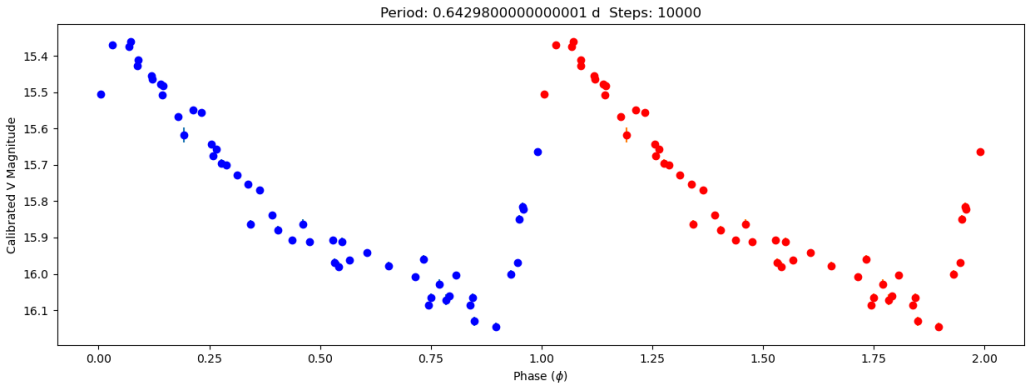

Figure 20: Apparent magnitude vs phase of V filter of S4.

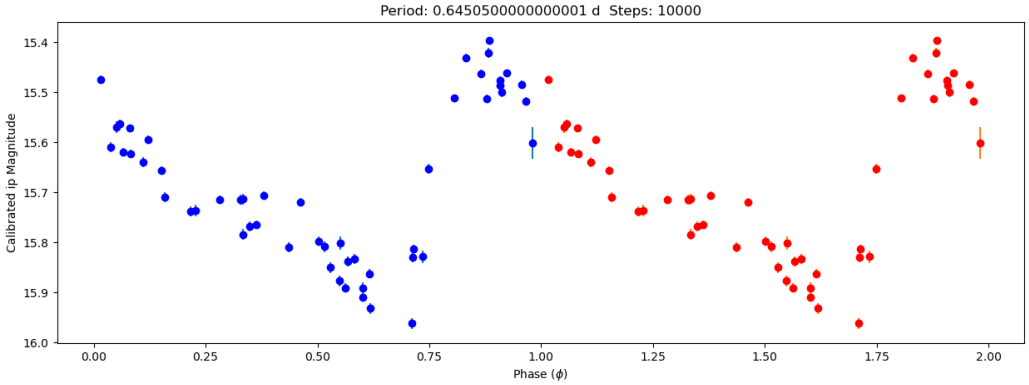

Figure 21: Apparent magnitude vs phase of i filter of S4.

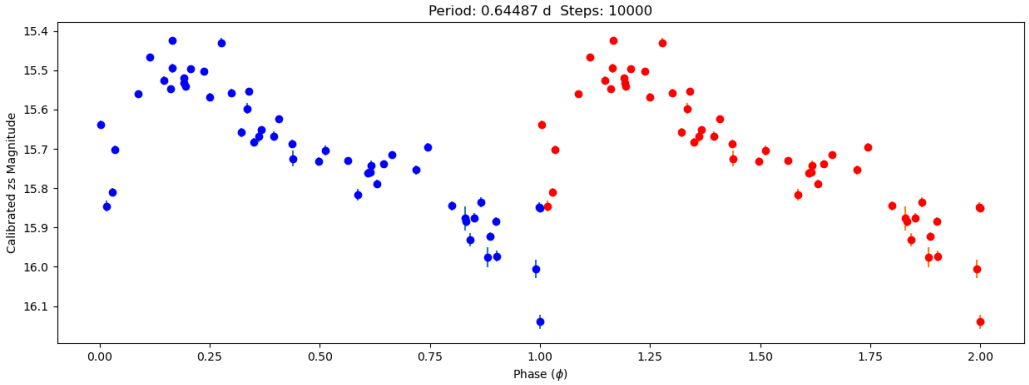

Figure 22: Apparent magnitude vs phase of z filter of S4.

Figures 23 through 25 show the V, i, and z apparent luminosity vs phase diagrams for S5. Due to steep curves and a period above .5 days, I determine S5 to be RRab.

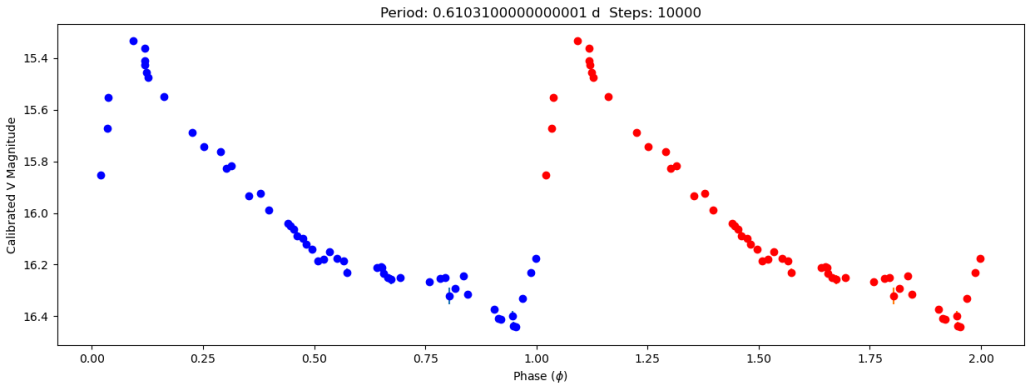

Figure 23: Apparent magnitude vs phase of V filter of S5.

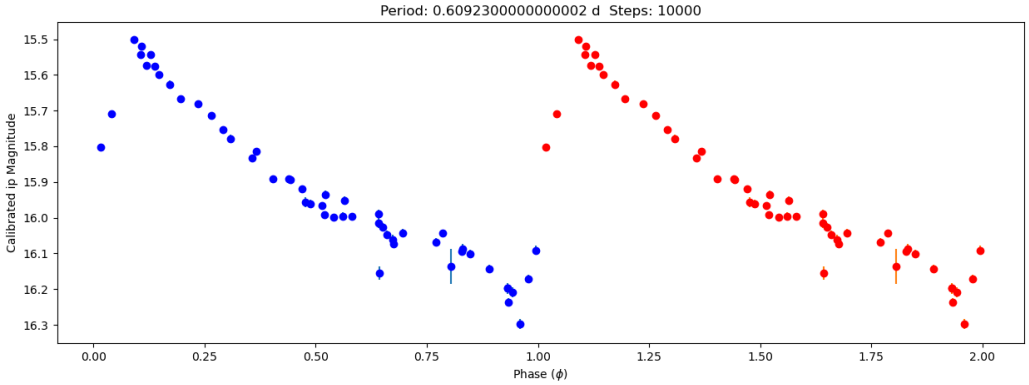

Figure 24: Apparent magnitude vs phase of i filter of S5.

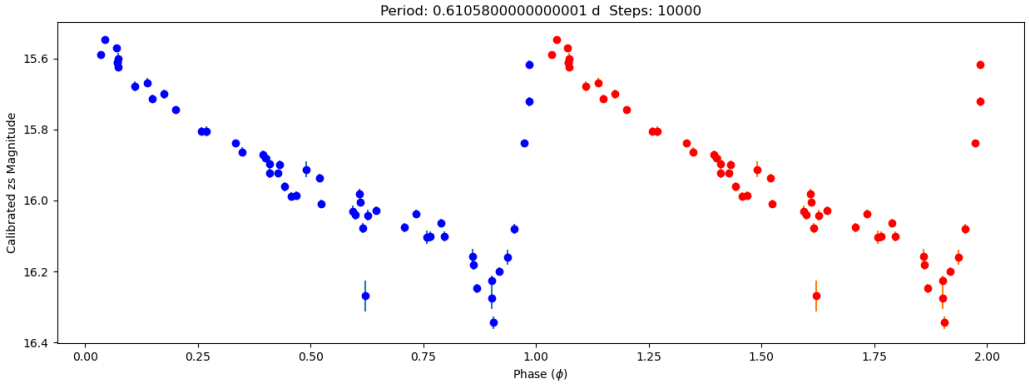

Figure 25: Apparent magnitude vs phase of z filter of S5.

Figures 26 through 28 show the V, i, and z apparent luminosity vs phase diagrams for star S6. Due to steep curves and a period above .5 days, I determine S6 to be RRab.

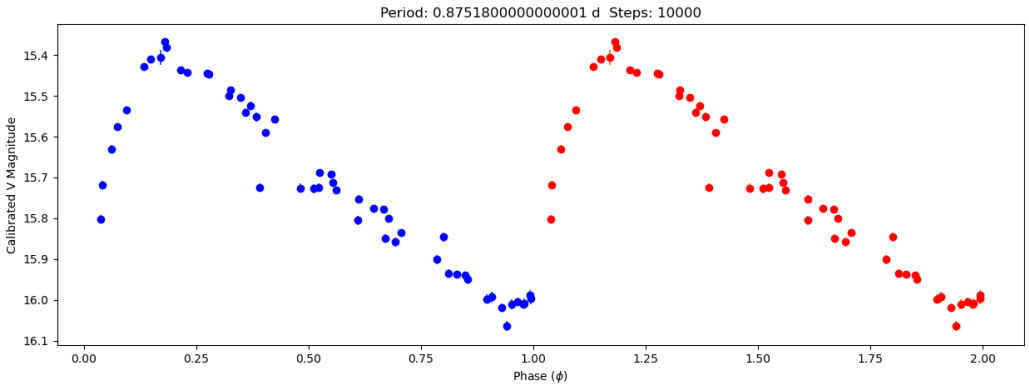

Figure 26: Apparent magnitude vs phase of V filter of S6.

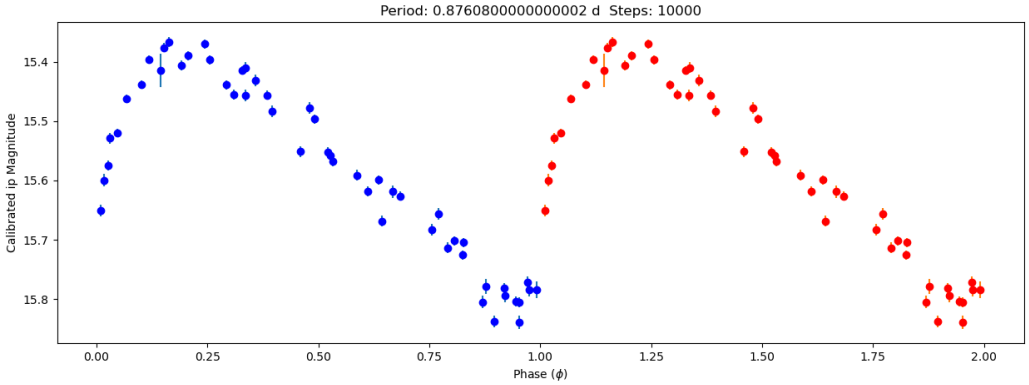

Figure 27: Apparent magnitude vs phase of i filter of S6.

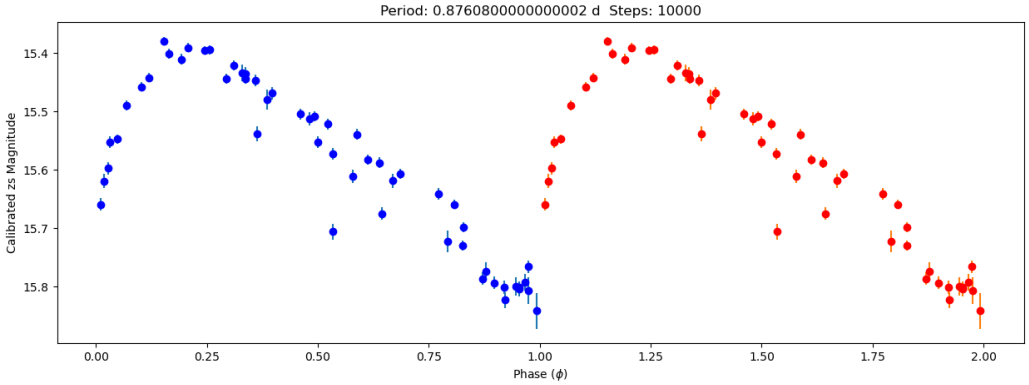

Figure 28: Apparent magnitude vs phase of z filter of S6.

Figures 29 through 31 show the V, i, and z apparent luminosity vs phase diagrams for S7. Due to steep curves and a period above .5 days, I determine S7 to be RRab.

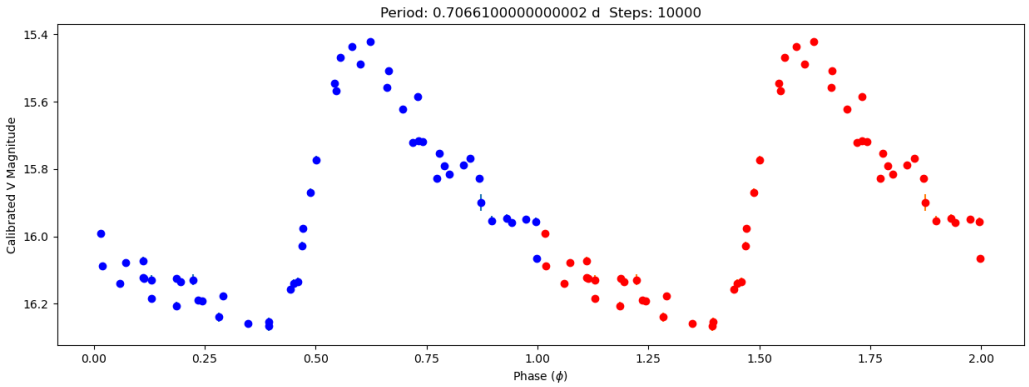

Figure 29: Apparent magnitude vs phase of V filter of S7.

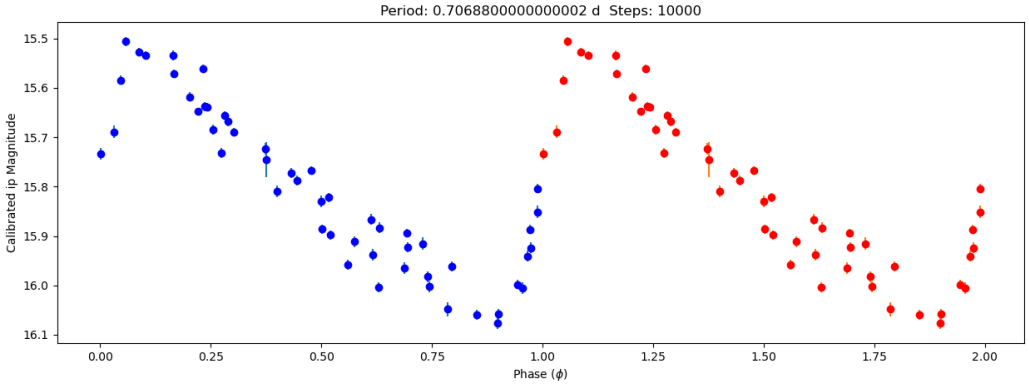

Figure 30: Apparent magnitude vs phase of i filter of S7.

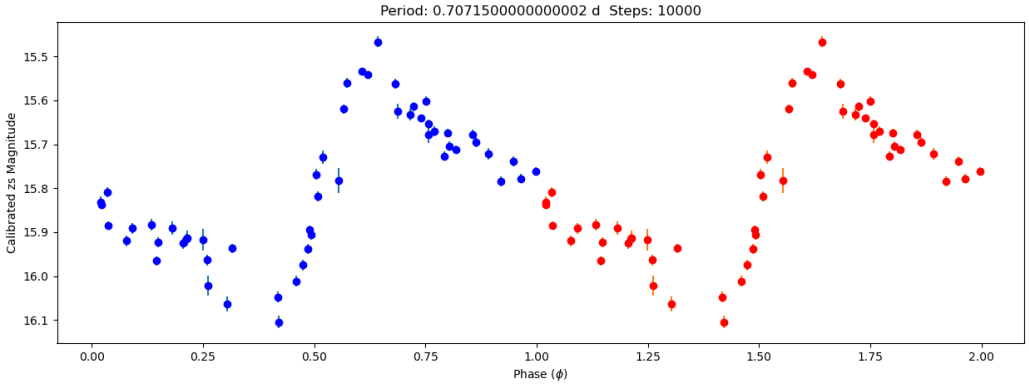

Figure 31: Apparent magnitude vs phase of z filter of S7.

Figures 32 through 34 show the V, i, and z apparent luminosity vs phase diagrams for S8. Due to steep curves and a period above .5 days, I determine S8 to be RRab.

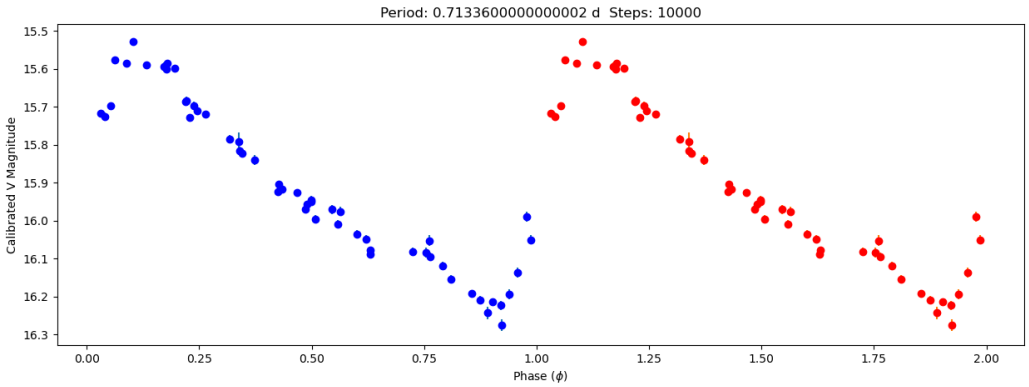

Figure 32: Apparent magnitude vs phase of V filter of S8.

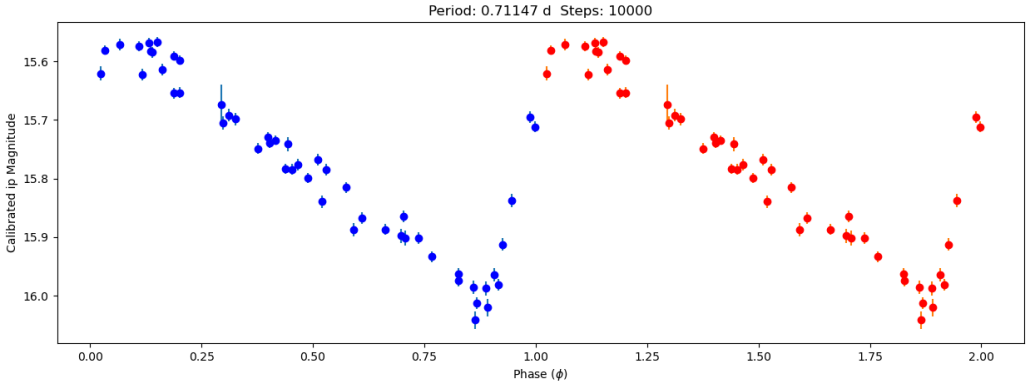

Figure 33: Apparent magnitude vs phase of i filter of S8.

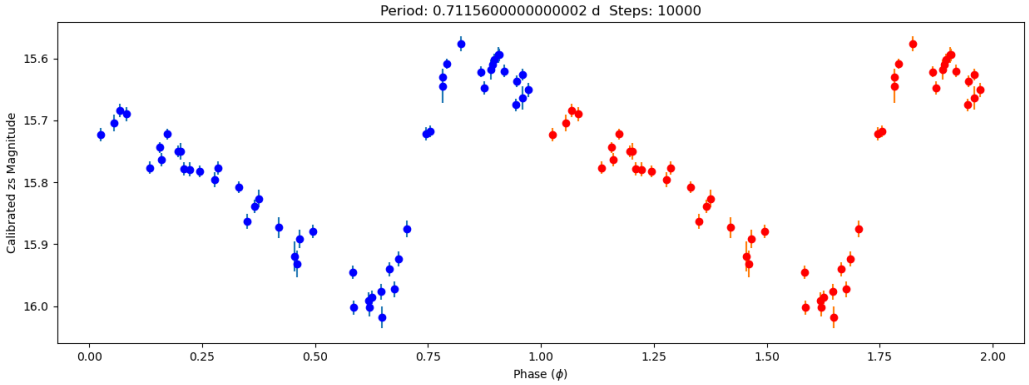

Figure 34: Apparent magnitude vs phase of z filter of S8.

Figures 35 through 37 show the V, i, and z apparent luminosity vs phase diagrams for S9. Due to sinusoidal curves and a period between .2 and .5 days, I determine S9 to be RRc. Figure 37 displays an irregular double period due to an outlier image that the algorithm did not reject. This is a product of the computational software and not a reflection of the star's behavior.

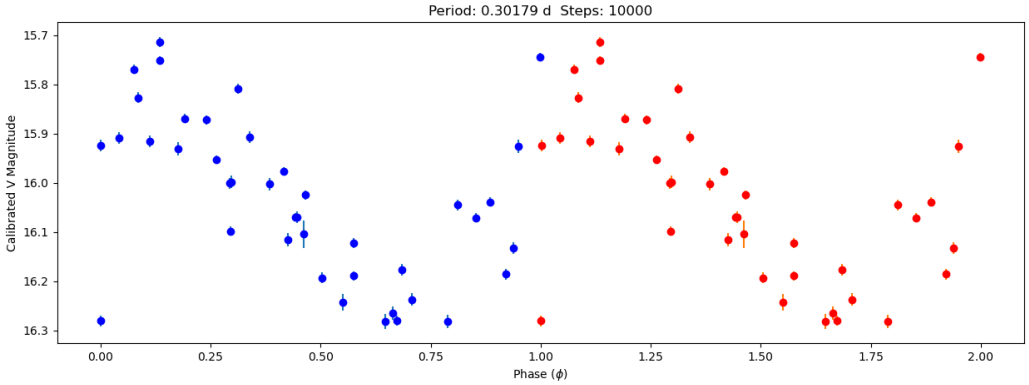

Figure 35: Apparent magnitude vs phase of V filter of S9.

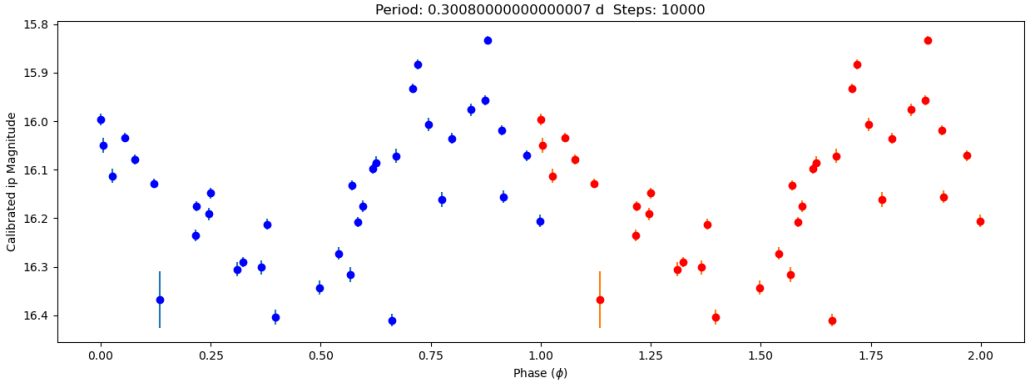

Figure 36: Apparent magnitude vs phase of i filter of S9.

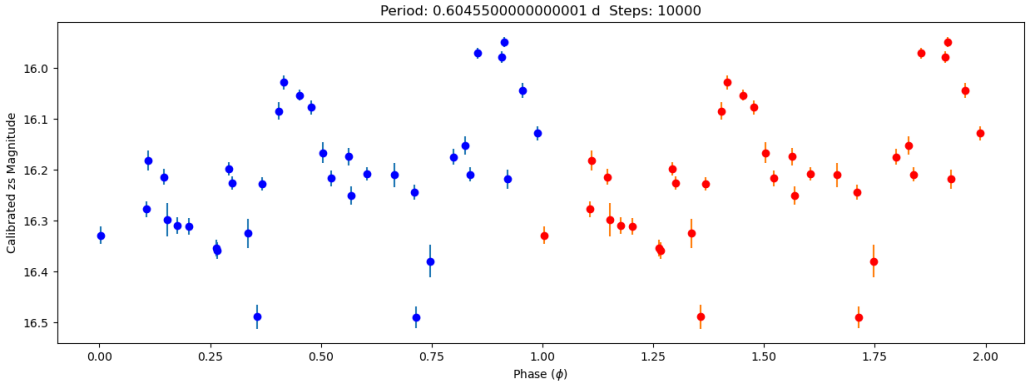

Figure 37: Apparent magnitude vs phase of z filter of S9.

Figures 38 through 40 show the V, i, and z apparent luminosity vs phase diagrams for S10. Due to sinusoidal curves and a period between .2 and .5 days, I determine S10 to be RRc.

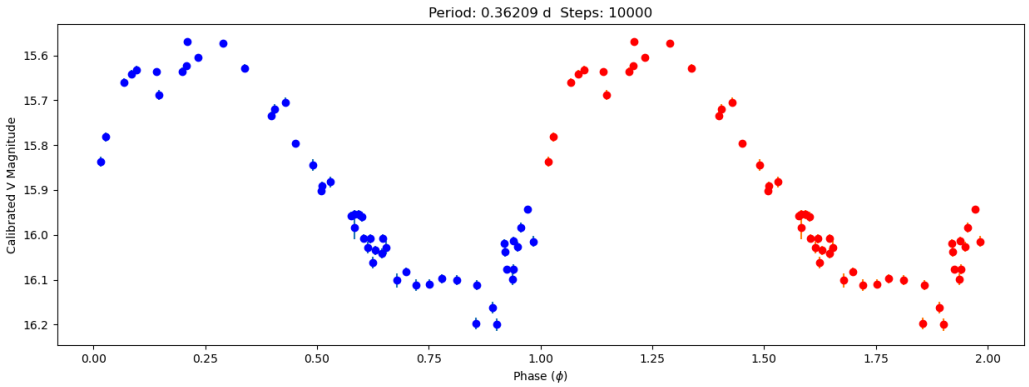

Figure 38: Apparent magnitude vs phase of V filter of S10.

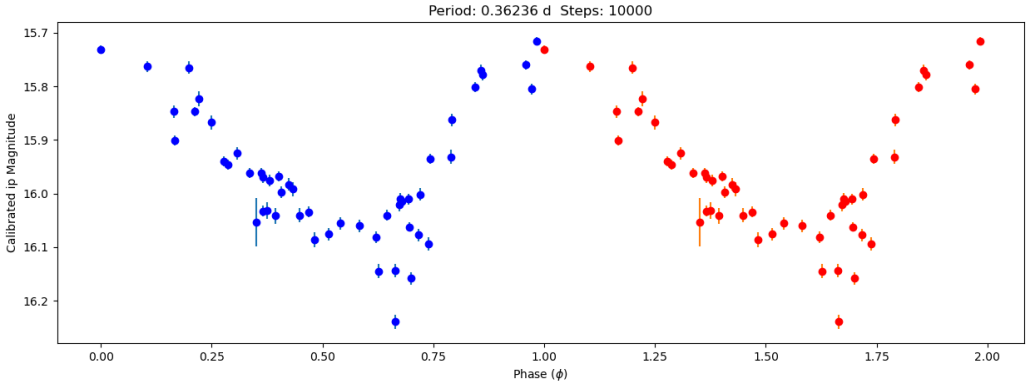

Figure 39: Apparent magnitude vs phase of i filter of S10.

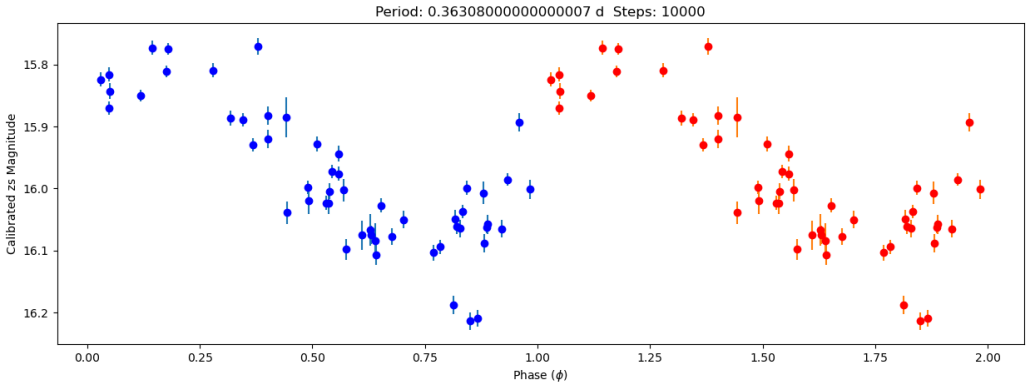

Figure 40: Apparent magnitude vs phase of z filter of S10.

Figures 41 through 43 show the V, i, and z apparent luminosity vs phase diagrams for S11. Due to sinusoidal curves and a period between .2 and .5 days, I determine S11 to be RRc.

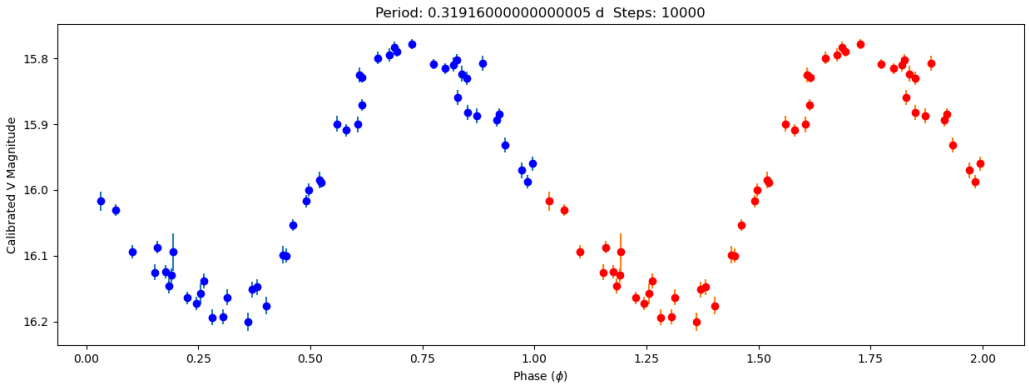

Figure 41: Apparent magnitude vs phase of V filter of S11.

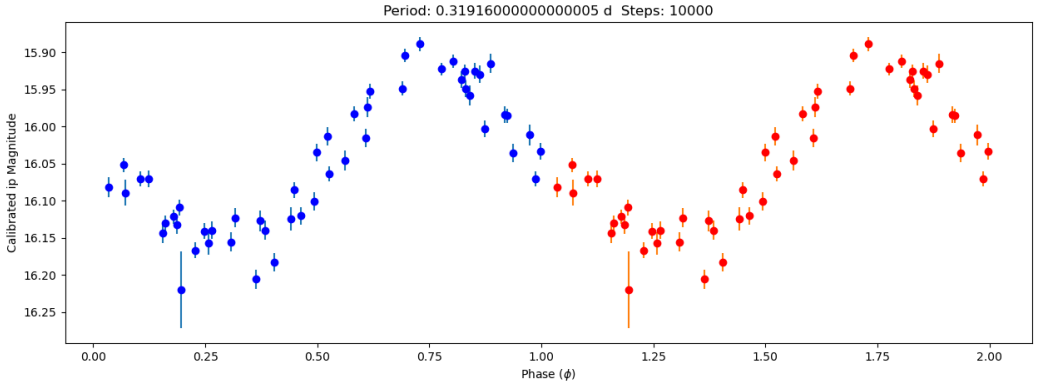

Figure 42: Apparent magnitude vs phase of i filter of S11.

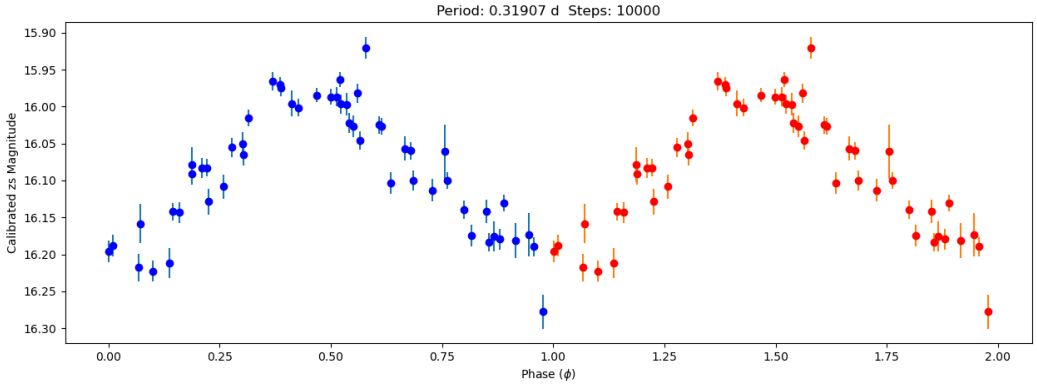

Figure 43: Apparent magnitude vs phase of z filter of S11.

Figures 44 through 46 show the V, i, and z apparent luminosity vs phase diagrams for S12. Due to sinusoidal curves and a period between .2 and .5 days, I determine S12 to be RRc. Figure 46 displays an irregular double period due to an outlier image that the algorithm did not reject. This is a product of the computational software and not a reflection of the star's behavior.

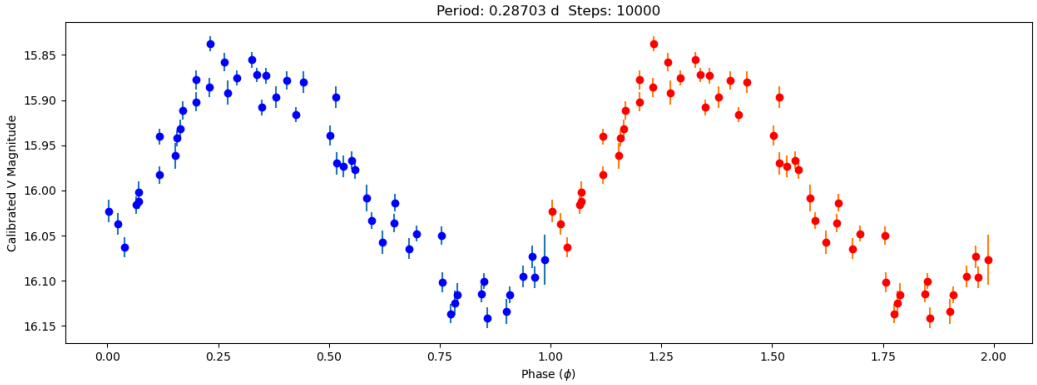

Figure 44: Apparent magnitude vs phase of V filter of S12.

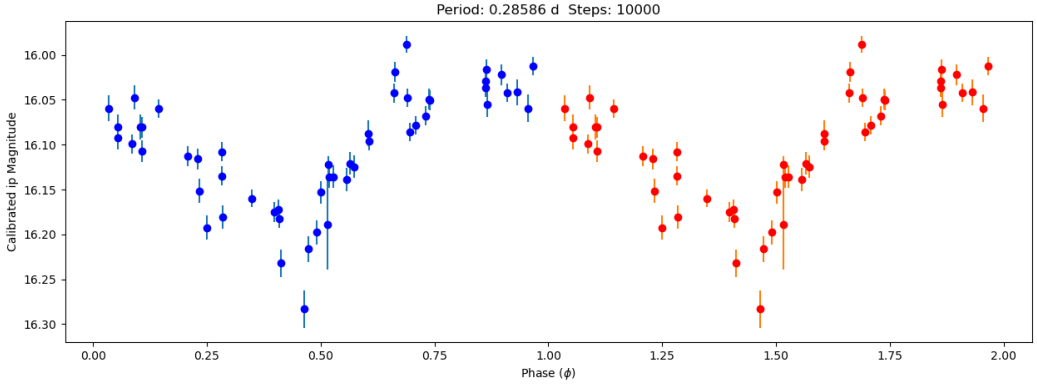

Figure 45: Apparent magnitude vs phase of i filter of S12.

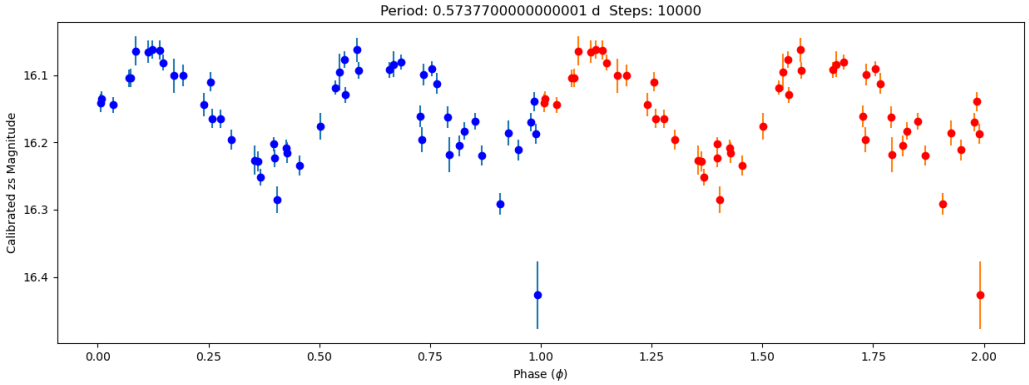

Figure 46: Apparent magnitude vs phase of z filter of S12.

Figures 47 through 49 show the V, i, and z apparent luminosity vs phase diagrams for S13. Due to sinusoidal curves and a period between .2 and .5 days, I determine S13 to be RRc. Figure 48 displays an irregular double period due to an outlier image that the algorithm did not reject. This is a product of the computational software and not a reflection of the star's behavior.

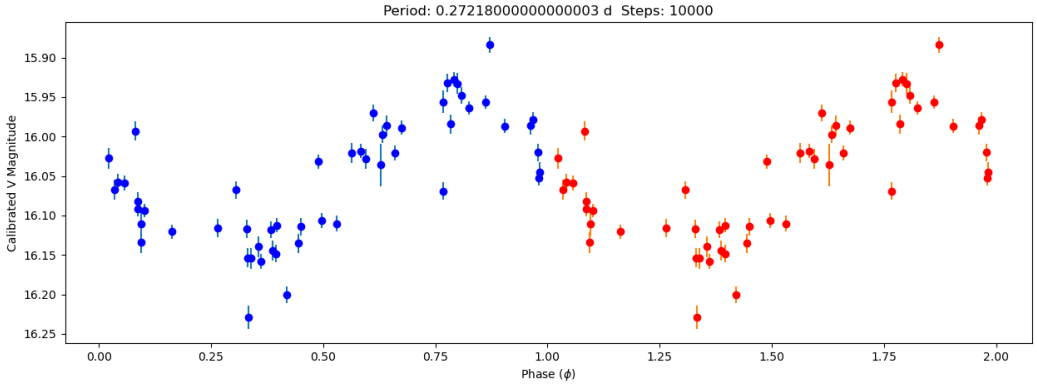

Figure 47: Apparent magnitude vs phase of V filter of S13.

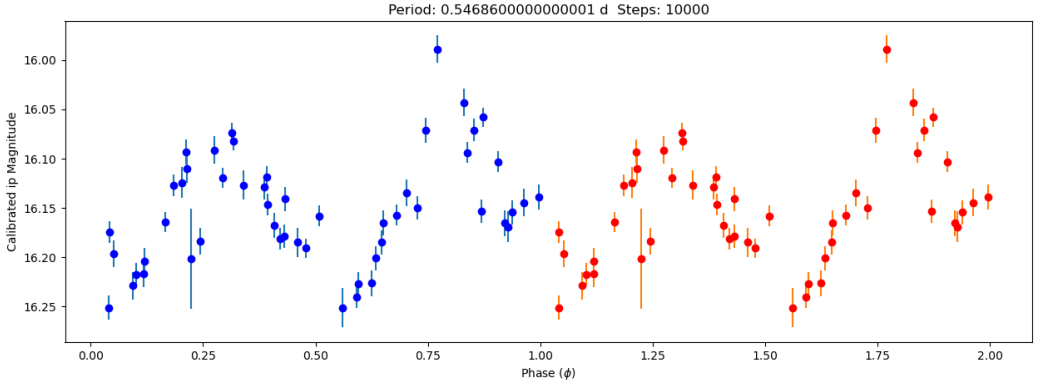

Figure 48: Apparent magnitude vs phase of i filter of S13.

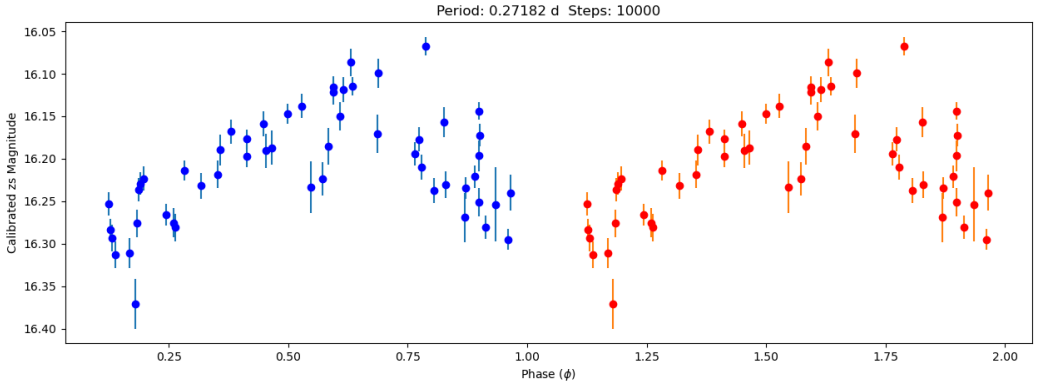

Figure 49: Apparent magnitude vs phase of z filter of S13.

Figures 50 through 52 show the V, i, and z apparent luminosity vs phase diagrams for S14. Due to sinusoidal curves and a period between .2 and .5 days, I determine S14 to be RRc. Figure 52 displays an irregular double period due to an outlier image that the algorithm did not reject. This is a product of the computational software and not a reflection of the star's behavior.

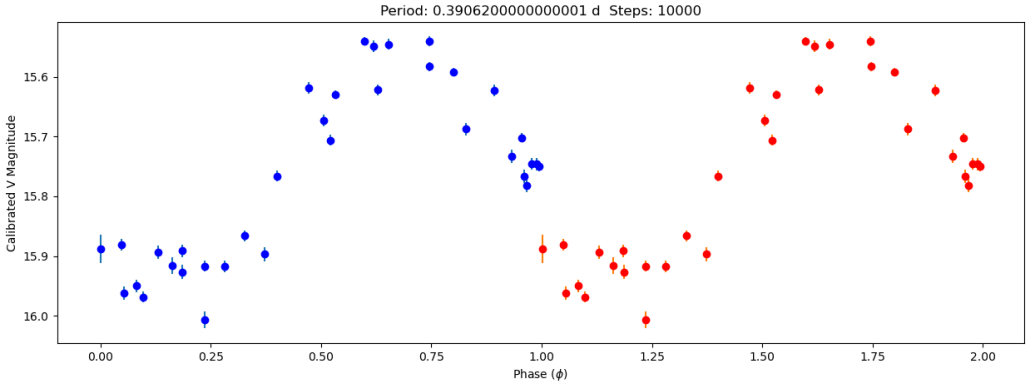

Figure 50: Apparent magnitude vs phase of V filter of S14.

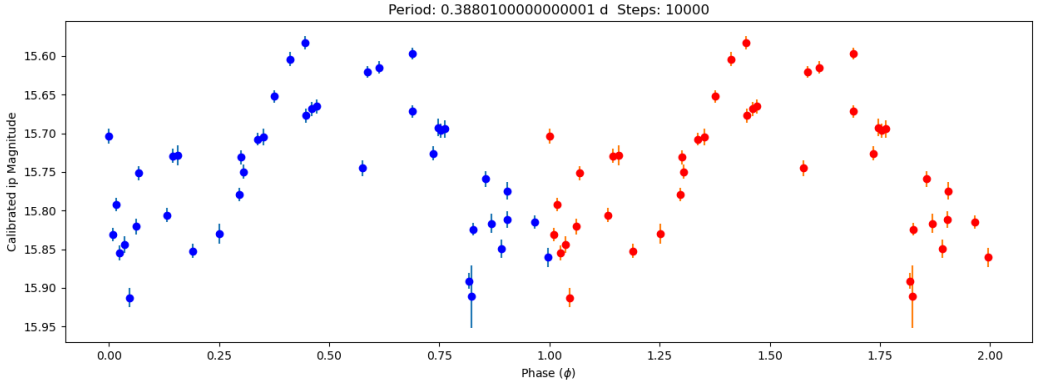

Figure 51: Apparent magnitude vs phase of i filter of S14.

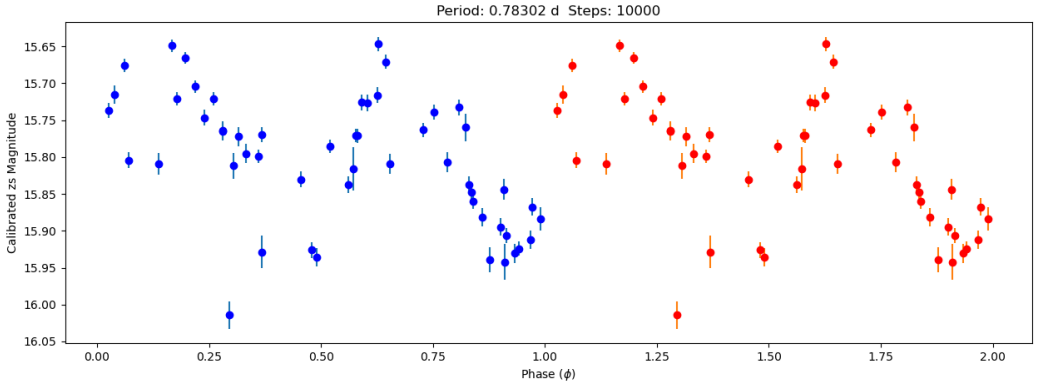

Figure 52: Apparent magnitude vs phase of z filter of S14.

Calculation and Results

We now examine the distance measurements calculated from the process described earlier. Since the pulsation period of the star is not dependent on filter type, for each star I use the periodicity obtained from the least noisy of the three filter plots. I determine which is least noisy by simply looking at the plots and using my best judgment. I apply the periods obtained from figures 10 through 51 to the distance calculation method described earlier. The metallicity of NGC 7089 to be used in absolute magnitude calculation for filters V, i, and z is published as [Fe/H] = -1.65. The color excess of NGC 7089 to be used to calculate the extinction factor, A, is published to be E(B-V) = 0.06[51]. The values for apparent magnitude are found to be the midline of the amplitude seen in the periodic light curves. Individual filter distance measurements, as well as total average distance across the three filters can be seen in Tables 1 and 2, respectively. The error in distance is calculated from a process that Michael Fitzgerald and I created due to the fact that a standardized periodicity error method does not exist. Error is calculated as a percentage of calculated distance, scaled based on star type and magnitude.

[51] Harris, “A Catalog of Parameters for Globular Clusters in the Milky Way.”

Star	Type	Period (days)	Distance (V) (pc)	Error (V) (pc)	Distance (i) (pc)	Error (i) (pc)	Distance (z) (pc)	Error (z) (pc)
S1	0	0.5294	9301.0	35	10980	31	10798	25
S2	0	0.61967	10435	39	11240	39	11751	35
S3	0	0.59492	10436	39	11250	36	11443	39
S4	0	0.64298	10059	38	10718	34	10947	28
S5	0	0.61031	10533	40	11733	38	12061	33
S6	0	0.87518	10035	38	11038	34	11325	28
S7	0	0.70661	10388	39	11552	34	11757	28
S8	0	0.71336	10679	40	11520	36	11748	30
S9	1	0.30179	11182	42	11820	116	12228	134
S10	1	0.36209	10606	40	11458	113	11614	128
S11	1	0.31916	11182	42	11686	115	11740	129
S12	1	0.38703	11157	42	11834	116	11960	131
S13	1	0.27218	11443	43	11772	116	11905	131
S14	1	0.39062	10012	38	10649	103	11000	118

Table 1: Distance measurements for each filter of all tracked stars. Type 0 refers to ab and type 1 refers to c, as is customary.

Star	Average Distance (kpc)	Average Error (kpc)
S1	10.360	0.0303
S2	11.142	0.0376
S3	11.043	0.0354
S4	10.575	0.0332
S5	11.442	0.0370
S6	10.800	0.0333
S7	11.232	0.0337
S8	11.316	0.0353
S9	11.743	0.0974
S10	11.226	0.0935
S11	11.536	0.0950
S12	11.650	0.0965
S13	11.706	0.0965
S14	10.554	0.0862

Table 2: Total average distance measurements across all 3 filters for all tracked stars.

The average pulsation period of the 8 RRab type stars is .66155d. The average pulsation period of the 6 RRc type stars is .33881d. Taking the distance average of the three filters of each star yields a grand total distance average of 11.483 kiloparsecs, with a standard deviation of 0.43332 kiloparsecs. Treating this distance average to be a measurement of the cluster distance as a whole, we see that the distance from Earth to NGC 7089 is 11.5 kpc, after accounting for significant figures derived from the error and metallicity used. Right ascension and declination can be seen in Table 3.

Star	RA	Dec
S1	323.3487	-0.80125
S2	323.4234	-0.83142
S3	323.404	-0.87294
S4	323.3429	-0.83653
S5	323.3135	-0.85658
S6	323.3864	-0.80972
S7	323.3398	-0.80086
S8	323.454	-0.76261
S9	323.3842	-0.84153
S10	323.3085	-1.01814
S11	323.4284	-0.96214
S12	323.4712	-0.79911
S13	323.3871	-0.80869
S14	323.3804	-0.83236

Table 3: Coordinates for tracked stars.

Discussion

The published distance measurement from the sun to the center of NGC 7089 is 11.5 kiloparsecs[52]. Comparing the RR Lyrae dataset analysis measurement I found to be 11.5 kiloparsecs, we see that the two values are the same within precision. The distance of 11.5 kpc published by Harris was calculated by examining 21 known RR Lyrae stars within NGC 7089 and undertaking the same process I used to calculate distance, but only in the V filter, using the same general metallicity and color gradient for the cluster.

By also using the i and z filter, along with the V filter, my method is a more rigorous and complete distance calculation. As can be seen in equations 5,6, and 7 the absolute magnitude for the V filter is dependent solely on metallicity, while the absolute magnitudes for the i and z filters depend on metallicity as well as pulsation period of the star. Because metallicity used is taken from the cluster as a whole, while the pulsation period is unique to each individual star, it can be assumed a measurement involving the pulsation period of a star will be a more robust method in estimating the distance to the star. Thus, the distance calculated from all three filters can be postulated to have a higher confidence level than the Harris catalog's distance measurement. This has a few implications due to my final distance measurement matching the Harris catalog. First, it gives reason to believe that distance calculations of globular clusters with similar metallicities and distances can be estimated with sufficient confidence by examining the cluster's RR Lyraes solely in the visible filter. For example, if a cluster is too far away from earth to be able to discern individual stars for a periodicity measurement, distance to the cluster can still be estimated with reasonable confidence using strictly metallicity. It also implies that using the metallicity of the cluster as a whole is generally sufficient for use in distance calculations for individual RR Lyraes within the cluster. These conclusions are beneficial scientific fallouts for the astronomy community. They are also novel given that a study of NGC 7089's RR Lyrae stars using the V, i, and z filters had not been performed and compared to the Harris catalog before this thesis project.

Putting this into more context than just the distance is evidence gathered relating to Oosterhoff type. As stated earlier, NGC 7089 is defined as a type II Oosterhoff globular cluster. Since type II clusters have RRab type stars with pulsation periods close to .64d, the average pulsation period of .66155d from the 8 analyzed RRab stars is confirming evidence that NGC 7089 is a type II Oosterhoff. Because NGC 7089 is a Milky Way cluster, an average RRab periodicity outside the range of .54d to .64d is expected in accordance with the Oosterhoff gap phenomena. Furthermore, 4 of the 8 RRab stars are above the .64d mark individually, while none of the other 4 RRab stars are below the .54d mark associated with Oosterhoff type I clusters. The r value within my sample (fraction of RRc to total RR stars measured) is seen to be .43. While a sample size of 14 does not provide the most accurate statistical model, it nevertheless shows evidence of type II Oosterhoff phenomena given that type II clusters have r values near .49, while type I clusters have r values close to .18 seen in equations 13 and 14. The published metallicity from Harris being [Fe/H] = -1.65 (less than the cutoff of [Fe/H] = -1.6) also corroborates the notion of NGC 7089 being Oosterhoff II. However, the published age of NGC 7089 is 12.5 billion years old, .5 billion years younger than the normal cutoff for type II clusters. This is unusual because statistically metallicity and age of globular clusters are directly related. An age of 12.5 Gyr would normally indicate a metallicity of around [Fe/H] = -0.5[53]. This

[52] Harris.
[53] van den Bergh, "Some Systematics of Galactic Globular Clusters."

anomaly is explained by a complicated metallicity based age calculation that is beyond the scope of this paper, but is explained in the Marín-Franch paper[54]. Aside from this anomaly, my data supports the claim of NGC 7089 being an Oosterhoff type II globular cluster.

Conclusion

From a measurement of 14 RR Lyrae variable stars within NGC 7089, a distance measurement of the globular cluster was found to be 11.5 kpc, matching that of the Harris catalog. The use of periodicity based distance estimates for the RR Lyrae stars lends this result to have a higher confidence level than the Harris catalog's. Because both methods yielded the same distance measurement, it is plausible to use strictly metallicity based distance calculations for globular clusters if periodicity inclusive methods are infeasible. To examine distance more accurately, spectroscopic measurements could be taken in order to discern metallicities for individual stars, rather than using metallicity of the cluster as a whole. My data supports the previously published notion that NGC 7089 is an Oosterhoff II cluster. This is prevalent due to an average RRab periodicity of .66155d, an r value of .43, and a metallicity of [Fe/H] = -1.65.

[54] Marin-Franch et al., "The ACS Survey of Galactic Globular Clusters. VII. Relative Ages."

Bibliography

"Astronomy 1101." Accessed March 17, 2022. https://www.astronomy.ohio-state.edu/thompson.1847/1101/lecture_evolution_low_mass_stars.html.

Bergh, Sidney van den. "Some Systematics of Galactic Globular Clusters." *Publications of the Astronomical Society of the Pacific* 123, no. 907 (2011): 1044–53. https://doi.org/10.1086/662132.

Cáceres, C., and M. Catelan. "The Period-Luminosity Relation of RR Lyrae Stars in the SDSS Photometric System." *The Astrophysical Journal Supplement Series* 179, no. 1 (November 2008): 242–48. https://doi.org/10.1086/591231.

Cardelli, Jason A., Geoffrey C. Clayton, and John S. Mathis. "The Relationship between Infrared, Optical, and Ultraviolet Extinction." *The Astrophysical Journal* 345 (October 1, 1989): 245. https://doi.org/10.1086/167900.

Carroll, Bradley, and Dale Ostlie. *An Introduction to Modern Astrophysics*. 2nd ed. University Printing House: Cambridge University Press, 2017.

Catelan, M., B. J. Pritzl, and H. A. Smith. "The RR Lyrae Period-Luminosity Relation. I. Theoretical Calibration." *The Astrophysical Journal Supplement Series* 154, no. 2 (October 2004): 633–49. https://doi.org/10.1086/422916.

Clement, Christine M., Adam Muzzin, Quentin Dufton, Thivya Ponnampalam, John Wang, Jay Burford, Alan Richardson, Tara Rosebery, Jason Rowe, and Helen Sawyer Hogg. "Variable Stars in Galactic Globular Clusters." *The Astronomical Journal* 122, no. 5 (November 2001): 2587–99. https://doi.org/10.1086/323719.

Dworetsky, M. M. "A Period-Finding Method for Sparse Randomly Spaced Observations or 'How Long Is a Piece of String?'" *Monthly Notices of the Royal Astronomical Society* 203, no. 4 (August 1983): 917–24. https://doi.org/10.1093/mnras/203.4.917.

"FeHcalculator.Pdf." Accessed March 10, 2022. http://www2.astro.puc.cl/pgpuc/data/FeHcalculator.pdf.

Fitzgerald, Michael. "Course: RR Course August 2020+." Accessed March 31, 2022. https://www.oursolarsiblings.com/moodle/course/view.php?id=22.

"Globular Cluster | Astronomy | Britannica." Accessed March 10, 2022. https://www.britannica.com/science/globular-cluster.

Granzer, Thomas. "Sloan u'g'r'i'z' Filter Curves — English." Page. Accessed March 24, 2022. https://old.aip.de/en/research/facilities/stella/instruments/data/sloanugriz-filter-curves.

Harris, William E. "A Catalog of Parameters for Globular Clusters in the Milky Way." *The Astronomical Journal* 112 (October 1996): 1487. https://doi.org/10.1086/118116.

"Horizontal Branch." In *Wikipedia*, April 28, 2021. https://en.wikipedia.org/w/index.php?title=Horizontal_branch&oldid=1020414602.

"Instability Strip." In *Wikipedia*, January 10, 2022. https://en.wikipedia.org/w/index.php?title=Instability_strip&oldid=1064832506.

Jurcsik, J., Á Sódor, B. Szeidl, Zs Hurta, M. Váradi, K. Posztobányi, K. Vida, et al. "The Konkoly Blazhko Survey: Is Light-Curve Modulation a Common Property of RRab Stars?" *Monthly Notices of the Royal Astronomical Society* 400, no. 2 (December 1, 2009): 1006–18. https://doi.org/10.1111/j.1365-2966.2009.15515.x.

Kuehn, Charles A., Horace A. Smith, Marcio Catelan, Young-Beom Jeon, James M. Nemec, Alistair R. Walker, Andrea Kunder, et al. "RR Lyrae in the LMC: Insights Into the Oosterhoff Phenomenon." *ArXiv:1310.0553 [Astro-Ph]*, October 1, 2013. http://arxiv.org/abs/1310.0553.

"LCO Filters Documentation." Accessed March 10, 2022.

https://lco.global/observatory/instruments/filters/.
Marin-Franch, Antonio, Antonio Aparicio, Giampaolo Piotto, Alfred Rosenberg, Brian Chaboyer, Ata Sarajedini, Michael Siegel, et al. “The ACS Survey of Galactic Globular Clusters. VII. Relative Ages.” *The Astrophysical Journal* 694, no. 2 (April 1, 2009): 1498–1516. https://doi.org/10.1088/0004-637X/694/2/1498.
“Modern Cosmological Observations and Problems - G. Bothun.” Accessed March 10, 2022. https://ned.ipac.caltech.edu/level5/Bothun2/Bothun2_3_2.html.
Netzel, Henryka, Radoslaw Smolec, Igor Soszynski, and Andrzej Udalski. “Blazhko Effect in the First Overtone RR Lyrae Stars of the OGLE Galactic Bulge Collection.” *Monthly Notices of the Royal Astronomical Society*, July 18, 2018. https://doi.org/10.1093/mnras/sty1883.
“OGLE Atlas of Variable Star Light Curves - RR Lyrae Stars.” Accessed March 10, 2022. http://ogle.astrouw.edu.pl/atlas/RR_Lyr.html.
Stobie, R. S. “On the Difference Between the Oosterhoff Types i and II Globular Clusters.” *The Astrophysical Journal* 168 (September 1971): 381. https://doi.org/10.1086/151094.
Zimmerman, Russell, Elene Bakhtadze, and Nicholas Dorogy. “New Distance and Period Estimates to OZ UMa, an RR Lyrae Star.” *Astronomy Theory, Observations and Methods Journal*, 2021.